General Disclaimer

One or more of the Following Statements may affect this Document

- This document has been reproduced from the best copy furnished by the organizational source. It is being released in the interest of making available as much information as possible.

- This document may contain data, which exceeds the sheet parameters. It was furnished in this condition by the organizational source and is the best copy available.

- This document may contain tone-on-tone or color graphs, charts and/or pictures, which have been reproduced in black and white.

- This document is paginated as submitted by the original source.

- Portions of this document are not fully legible due to the historical nature of some of the material. However, it is the best reproduction available from the original submission.

INVESTIGATION OF SEPARATION AND THE ASSOCIATED

HEAT-TRANSFER AND PRESSURE DISTRIBUTION

ON CONE-CYLINDER-FLARE CONFIGURATIONS

AT MACH 5

By John W. Schaefer and Harold Ferguson

Lewis Research Center
National Aeronautics and Space Administration
Cleveland, Ohio

INVESTIGATION OF SEPARATION AND THE ASSOCIATED

HEAT-TRANSFER AND PRESSURE DISTRIBUTION

ON CONE-CYLINDER-FLARE CONFIGURATIONS

AT MACH 5

By John W. Schaefer and Harold Ferguson

Lewis Research Center
National Aeronautics and Space Administration
Cleveland, Ohio

SUMMARY

The separated region across the cylinder-flare junction of a cone-cylinder-flare configuration and its effect on the overall heat-transfer and pressure distributions were investigated at a Mach number of 4.98. Results are presented for pure laminar and transitional separation and for both laminar and turbulent attached flow on a 15° half-angle cone-cylinder model with conical flare afterbodies of 10°, 17°, 24°, and 56° half-angles. The free-stream unit Reynolds number ranged from 1.6×10^6 to 5.4×10^6 ft^{-1} and the wall temperature from $T_w/T_{aw} = 0.18$ to 1.0.

The extent of a pure laminar separation and a transitional separation was found to decrease with wall cooling, decreasing flare angle, and increasing unit Reynolds number. The heat transfer at reattachment and downstream was dependent on the type of separation - pure laminar or transitional. Low heat-transfer rates were found downstream of a pure laminar separation. For transitional separation, the heat transfer downstream of reattachment was at the high values associated with a thin turbulent boundary layer, with peak heating in the vicinity of reattachment.

INTRODUCTION

Aerodynamic considerations of a reentry vehicle dictate a body geometry that may result in regions of extensive separated flow. The existence of a separated region may appreciably reduce the expected vehicle drag and greatly increase the heat transfer downstream of the separated region. Therefore, the effect of flow separation on pressure distribution and, in particular, on heat transfer is of importance. The influence of such parameters as Reynolds number, Mach number, wall temperature, and vehicle geometry on the onset, type, and extent of separation is therefore necessary.

Three distinct flow separation regimes have been recognized and classified by Chapman, Kuehn, and Larson (1).[1] They are: pure laminar separation where transition occurs downstream of reattachment, transitional separation where transition occurs between separation and reattachment, and turbulent separation where transition is upstream of separation. The pressure distribution across a separated region was found to be dependent on the type of separation -. pure laminar, transitional, or turbulent.

A theoretical investigation of heat transfer in regions of laminar separation and turbulent separation where the boundary-layer thickness at separation is small or zero was presented by Chapman (2). The average heat transfer in a region of pure laminar separation was found for air to be 0.56 that of the corresponding attached flow on a solid boundary defined by the edge of the separated region. The average heat transfer in a region of turbulent separation, however, was found to be higher than the corresponding attached flow and to be strongly dependent on Mach number, decreasing with increasing Mach number. Larson (3), in an experimental investigation of separation heat transfer on a model that approximated the theoretical model of Chapman, found good agreement between experiment and theory for pure laminar separation. For turbulent separation, however, the average heat transfer was found to be less than that for the corresponding attached flow and essentially independent of Mach number. The distribution of heat transfer across the separated region was also presented.

The heat transfer in the reattachment region has also generated considerable interest. The available results include experimental wind tunnel and free·flight investigations carried out by the Langley Research Center (classified) and the investigations of (4 to 6). The reported heat-transfer rates in the reattachment region ranged from low values to very high values. Crawford (5), based on his results and those of (4) for separation induced by a spike on the nose of a hemisphere-cylinder, suggests that the reattachment heat transfer may be strongly dependent on the type of separation.

Larson and Keating (7) investigated the transition Reynolds number for cylindrical separations on an ogive-stepped cylinder model on which the separation length was controlled. The transition Reynolds number was defined as the maximum Reynolds number, based on the length of separation, for which laminar flow existed throughout the separated region. They presented results for Mach numbers up to 4.24 and for adiabatic and cold wall conditions. The transition Reynolds number was found to increase with increasing Mach number, unit Reynolds number (Re/ft), and wall temperature. A marked effect of the wall temperature level upstream of separation was also apparent.

---

[1]Numbers in parentheses indicate References at end of paper.

In this paper results are presented for the separated region across the cylinder-flare junction of a cone-cylinder-flare configuration and its effect on the heat-transfer and pressure distributions at a Mach number of 4.98. The effects of flare angle, wall cooling, and Reynolds number on the geometry of the separated region are presented for pure laminar and transitional separations. The overall heat-transfer and pressure distributions are presented for each separation type and for a turbulent attached flow with no separation. The free-stream unit Reynolds number ranged from 1.6×10^6 to 5.4×10^6 ft^{-1}, the wall temperature from $T_w/T_{aw} = 0.18$ to 1.0, and the flare angles were $\theta = 10^O$, 17°, 24°, and 56°. Transition occurred naturally and was induced by a trip on the model nose cone.

TEST PROCEDURE AND DATA REDUCTION

Tests were conducted in the Lewis Research Center 1- by 1-foot Mach 5 variable Reynolds number wind tunnel. The air stagnation temperature was constant at 710 R. The test model was a thin-wall Monel cone-cylinder-flare configuration. The interchangeable flare afterbodies had half-angles of 10°, 17°, 24°, and 56°. Model dimensions are shown in Fig. 1. A typical tunnel installation with the model in test position is shown in Fig. 2. Two test series were run: one where transition occurred naturally, and one where transition was induced by a boundary-layer trip on the model nose cone. The trip, shown in Fig. 1, was a 1/8-in. band of granulated nickel glued to the model with epoxy cement.

Heat-transfer data were obtained by the transient technique developed in (8). The model was enclosed in the cooling shoes and cooled with liquid nitrogen to an approximately uniform temperature of 120 R before introducing it into the tunnel stream. Heat-transfer data were evaluated from the familiar thin-wall analysis presented in (8). The heat-transfer coefficient for negligible wall conduction and radiation is given by

$$h = \frac{\rho_b (c_p)_b \tau_w \frac{dT_w}{dt}}{T_{aw} - T_w} \qquad [1]$$

The specific heat variation for Monel is presented in (8). The wall temperatures were determined from oscillograph records at discrete times and equal time intervals, and the rate of change of temperature with time was determined by differentiation of a five-point quadratic fit of the experimental temperatures. The experimental adiabatic wall temperatures were used in the calculations.

Model static and the tunnel static pressures were read on a butyl phthalate and mercury manometer board. Pressure distribution results were obtained for equilibrium conditions only. For the purpose of correlating the pressure distributions across the separated region, a curve was faired through the experimental points. At low unit Reynolds numbers ($Re/ft \leq 2.6 \times 10^6$), however, the manometer-system settling time in regions of low pressure was found to be prohibitive. Therefore, the pressure distributions across the separated region at low unit Reynolds numbers were approximated by fairing a curve from a high pressure point in the separated region (which should be accurate) to the theoretical attached flow value upstream of separation with the measured experimental points as a guide.

Schlieren photographs were taken at intervals throughout each transient (heat-transfer) test and at all equilibrium conditions.

The classification of separation types was accomplished from study of schlieren photographs and heat-transfer results. In some cases for which transition was in the vicinity of reattachment, it was difficult to pinpoint the location of transition and therefore to distinguish between pure laminar and transitional separations. Since in these cases transition was in the immediate vicinity of reattachment and therefore in what may be termed the reattachment region, they are classified as transitional separations.

The estimated accuracy of the variables required for data reduction is as follows:

Wall thickness, τ_w, percent . . . . ±2
Wall material specific heat, $(c_p)_b$, percent . . . . ±3
Wall temperatures
    Adiabatic, R . . . . ±2
    High temperature range, R . . . . ±2
    Low temperature range, R . . . . ±4
Stagnation temperature, R . . . . ±2
Stagnation pressure, percent . . . . ±1
Static pressure (except as noted at low Reynolds number
   previously), percent . . . . ±3

The largest sources of possible error in the heat-transfer coefficient, Eq. [1], is the slope dT_w/dt and the temperature difference $T_{aw} - T_w$. The inaccuracy in the heat-transfer results is therefore greatest at low unit Reynolds number (where dT_w/dt was small) and at high wall temperature (where both $T_{aw} - T_w$ and dT_w/dt were small). The heat-transfer results presented are felt to be accurate within ±20 percent except for those experimental points indicated by a broken symbol for which the possible error is greater. These points are included only to give an indication of the low heat transfer in the separated region.

RESULTS AND DISCUSSION

The presentation of results that follows is divided into sections according to the location of the point of separation. All results for separation of the attached flow on the cylinder, which represent the major part of the investigation, are presented in the section "Cylinder Boundary-Layer Separation." For large flare angle ($\theta = 56^{\circ}$), separation occurred in the nose cone boundary layer and was markedly different from that obtained for separation at smaller flare angles. These results are treated in the section "Nose Cone Boundary-Layer Separation." The turbulent results obtained by tripping the boundary layer on the nose cone exhibited negligible separation and are presented in the section "Tripped Boundary Layer."

Cylinder Boundary-Layer Separation

Separation types. -- Pure laminar separation, shown in Fig. 3, occurred only for the minimum flare angle, $\theta = 10^{\circ}$, at unit Reynolds numbers below approximately 2.6×10^6 ft^{-1}. The boundary layer appears continuous through reattachment and remains laminar until transition occurs in the attached flare boundary layer. The small unit Reynolds number range for which results are available did not allow determination of the effect of unit Reynolds number on the location of transition. A stabilizing effect on the attached laminar boundary layer on the flare due to wall cooling was apparent over the wall temperature range for which schlieren photographs are available, $0.27 < T_w/T_{aw} \leq 1.0$. Observation of this effect from heat-transfer results was not possible because of a malfunction of the two thermocouples in the region over which transition moved. This trend agrees with the results of Jack and Diaconis (8) for moderate wall cooling.

Transitional separation, shown in Fig. 4, was observed for the 10° flare at unit Reynolds numbers above approximately 3.6×10^6 ft^{-1} and for all other flare angles at all unit Reynolds numbers. The start of transition is in the vicinity of reattachment for the large range of variables for which a transitional separation of the cylinder boundary layer occurred. The reattachment shock - boundary-layer interaction is apparently such that transition is triggered in the vicinity of reattachment for a large range of conditions and the attached turbulent or transitional boundary layer is quite thin downstream of reattachment. It is interesting to note that the Reynolds number based on separation length shows the same trends with unit Reynolds number and wall cooling (decreasing Re_l with wall cooling and decreasing unit Reynolds number) as

the transition Reynolds number for a separated flow from Larson and
Keating (7). It is therefore possible that the Reynolds number based on
separation length is approximately equal to the corresponding transition
Reynolds number at all test conditions for which transitional separation
occurred.

The approximate unit Reynolds number range on the 10° flare,
$2.6 \times 10^6 \leq \mathrm{Re/ft} \leq 3.6 \times 10^6$, is the range in which it was difficult to
distinguish between a pure laminar and a transitional separation and in
which both types may occur, depending on wall temperature. The corre-
sponding transition Reynolds number (based on free-stream conditions)
lies in the range $0.86 \times 10^6 < \mathrm{Re}_{TR} \leq 0.97 \times 10^6$ for adiabatic conditions,
where the transition Reynolds number is defined as the maximum Reynolds
number, based on free-stream conditions and the length of separation,
for which laminar flow exists throughout the separated region. It was
not possible to determine the wall temperature effect on the transition
Reynolds number because of insufficient data.

The model configuration and test conditions were such that no tur-
bulent separation results were obtained; transition did not occur natu-
rally in the attached cylinder boundary layer and, in the tripped case
discussed later, the extent of turbulent separation was negligible.

Separation geometry. - The variables defining the geometry of the
separated region are shown in Fig. 5. The point of separation s_s or
x_s is taken as the point at which the boundary layer begins to thicken
because of separation. The point of reattachment s_r or x_r is taken
as the intersection of the extension of the line that delineates the
edge of the separated region with the flare surface.

The edge of the separated region is defined by an essentially
straight line as seen in Figs. 3 and 4. At constant test conditions no
fluctuation in the locations of the points of separation and reattachment
was apparent. The separation angle α for separation of the attached
cylinder boundary layer was constant at approximately 3° independent of
type of separation (pure laminar or transitional), flare angle, unit
Reynolds number, and wall cooling. Fastax schlieren movies revealed a
small high-frequency flow fluctuation in the reattachment region for
transitional separation that was not apparent from visual observation of
the schlieren screen.

The extent of the separated region varied considerably for the range
of variables of the investigation. The length of separation l decreased
with decreasing flare angle, with wall cooling, and with increasing unit
Reynolds number; each effect is apparent from Fig. 4. The type of sepa-
ration, pure laminar or transitional, had no apparent influence on the
geometry over the range of variables in this investigation. The varia-
tion of separation length with unit Reynolds number is presented in

Fig. 6(a). A decrease in unit Reynolds number from 5.4×10^6 to 1.6×10^6 ft^{-1} results in an increase in the length of separation by a factor slightly greater than 2. The increase in the extent of separation with increasing flare angle is apparent from the figure. The corresponding plot of distance to separation is presented in Fig. 6(b).

All cold wall separation length results on the 24° flare, the only flare angle for which extensive results are available, are presented in Fig. 7 in terms of the measured adiabatic separation length. The length of separation decreases by a factor of about 2 as the wall temperature is reduced from adiabatic to $T_w/T_{aw} = 0.2$. Moderate cooling has little effect on the length of separation; appreciable reduction occurs only below $T_w/T_{aw} \doteq 0.5$. No consistent unit Reynolds number effect is apparent. The available results on the 10° and 17° flares exhibit the same trend. Visual schlieren observations also indicated that an increase in wall temperature above adiabatic resulted in an increase in the length of separation over the corresponding adiabatic wall value.

Pressure distribution. - Representative equilibrium pressure distributions in terms of the pressure coefficient C_p are presented in Figs. 8 and 9 for pure laminar and transitional separation, respectively. The theoretical attached flow pressure distribution for the cone-cylinder forebody from (11) is included in the figure. Ideally, the flare pressure distribution should decrease uniformly from the two-dimensional value at the cylinder-flare junction to the conical value downstream (12). Therefore, both the wedge pressure coefficient and cone pressure coefficient (13) for the flares are presented in the figures. The wedge and cone pressure coefficients for the approximate separation angle, $\alpha = 3^\circ$, are also included.

The pressure distribution for the attached flow on the cone-cylinder agrees favorably with theory (except as noted previously at low unit Reynolds number) until separation begins to influence the distribution at a point slightly upstream of separation. Between the start of interaction s_0 and the cylinder-flare junction, the pressure increases above the corresponding attached flow value and, as seen in Fig. 9(b) for larger separation lengths, levels off to a plateau pressure upstream of the cylinder-flare junction. As seen in the figures, the plateau pressure falls between that for a cone and that for a wedge at the approximate angle defined by the edge of the separated region ($\alpha = 3^\circ$). The start of the pressure jump associated with the flare afterbody occurs close to the cylinder-flare junction for separation of the cylinder boundary layer, independent of separation type. This behavior is in contradistinction to the two-dimensional separation results of (1), in which the pressure jump occurred at reattachment for a pure laminar separation and at transition for a transitional separation. The pressure jump in the vicinity of the cylinder-flare junction reaches a value

8

between that for a wedge and that for a cone (at the flare angle), and approaches the cone value downstream as expected (12).

Chapman, Kuehn, and Larson (1) determined that the pressure distribution across a separated region is well correlated for a pure laminar separation and for a transitional separation up to the start of transition by a plot of $(p/p_0 - 1)/\sqrt{(C_f)_0}$ against $(s/s_0 - 1)/\sqrt{(C_f)_0}$, where the subscript 0 indicates the start of interaction of separation on the pressure distribution. The correlation is presented in Fig. 10 for all faired, separated region pressure distribution results up to the start of the pressure jump in the vicinity of the cylinder-flare junction. The shaded area represents the range of the faired results. The plateau pressure for two-dimensional separations has been investigated in (1) at Mach numbers lower than that of this investigation. From these results (1) and the Mach number effect determined from the analysis of (1), the two-dimensional pressure plateau parameter $(p_p/p_0 - 1)/\sqrt{(C_f)_0}$ at Mach 5 may be determined. This computed value is approximately 18 as compared with the value for the three-dimensional separations of this investigation (Fig. 10) of approximately 21.

Heat transfer. - Representative overall heat-transfer distributions in terms of $St-\sqrt{Re_D}$ for pure laminar separation and for transitional separation are presented in Figs. 11 and 12, respectively. The laminar attached flow theory of Cohen and Reshotko (9 and 10) for the entire model and the turbulent theory of Reshotko and Tucker (14) for an attached turbulent boundary layer starting with zero thickness at the cylinder-flare junction are shown for comparison. In each case the theoretical curves were determined for the isothermal wall temperatures indicated. The pressure distribution assumed was the theoretical distribution for attached flow on the cone-cylinder and the cone pressure corresponding to the flare angle for the flares except as noted specifically in the figures. Where possible, the experimental separation and reattachment points from schlieren photographs are included for the heat-transfer and wall temperature distributions presented.

As seen in Figs. 11 and 12, the experimental heat transfer for the attached flow on the nose cone and cylinder is consistently higher than theory. The results are too consistent to attribute the discrepancy entirely to experimental error. A possible explanation of the discrepancy is the effect of the nonuniform wall temperature. The correction of the theory for the nonisothermal wall temperature distribution, discussed in (8), was not performed; however, it would be expected to bring theory closer to experiment. In general, the laminar attached flow results agree favorably in trend with the wall temperature effect predicted by isothermal theory as shown in Fig. 11.

Because of the larger possible inaccuracies in the separated region heat-transfer results, the effects of nonuniform wall temperature, and the limited number of data stations in the separated region, a definitive discussion of the heat transfer in the separated region is not possible. Observations from study of all available results deserve comment, however. The separated region heat transfer upstream of the cylinder-flare junction falls below that which would be expected for a laminar attached flow, based on extrapolation of the upstream attached flow results. The magnitude of the experimental decrease, however, is not as great as would be expected from the results of (2) and (3) for laminar separation with small or zero boundary-layer thickness at the point of separation. The minimum heat transfer occurs in the vicinity of the separation point x_S, and the region of low heat transfer is quite small compared with the extent of separation. The heat transfer increases sharply upstream of reattachment or transition and, in fact, upstream of the cylinder-flare junction.

A comparison of the heat-transfer distributions at reattachment and downstream in a pure laminar separation and a transitional separation, Figs. 11 and 12, demonstrates the significance of separation type on flare heat transfer. For transitional separation, the heat-transfer rates at reattachment and downstream are high, with peak heating in the vicinity of reattachment, and, as observed from schlieren photographs, reflect the transition to a thin turbulent boundary layer in the reattachment region. Turbulent theory, assuming a turbulent boundary layer starting with zero thickness at the cylinder-flare junction, adequately predicts the attached flow heat transfer on the flare for the transitional separations. For pure laminar separation the heat-transfer distribution downstream of reattachment (but upstream of transition) agrees favorably with laminar theory in trend, although it is somewhat above it in magnitude, indicating, as observed from schlieren photographs, a continuous laminar boundary layer through reattachment.

The equilibrium temperature distributions, included with the heat-transfer results, Figs. 11 and 12, demonstrate a rise across the separated region that begins somewhat upstream of the point of separation. For both pure laminar and transitional separation the peak in the distribution occurs in the vicinity of transition.

Nose Cone Boundary-Layer Separation

Separation induced by a large angle flare, 56° half-angle, was markedly different from the separation discussed previously, as seen in the schlieren photograph of Fig. 13. No attached flow occurs on the cylinder, separation occurs directly off the model nose cone, and no distinct reattachment point is apparent. The entire model downstream of the cone-cylinder junction is immersed in a separated flow. The

separation is transitional with transition just downstream of the point
of separation. The distance to transition decreases with wall cooling
as shown in Fig. 14. The separation angle α is approximately 10° in-
dependent of wall cooling, and is approximately the angle defined by
the line connecting the cone-cylinder junction and the tip of the flare.
Results are presented only at a unit Reynolds number of 5.4×10^{6} ft^{-1}
because tunnel blockage and the shock pattern off the model were such
that it was impossible to obtain a clean supersonic flow at lower unit
Reynolds numbers.

The equilibrium pressure distribution is presented in Fig. 13. The
distribution is considerably higher than that expected for an attached
flow on the cylinder. The agreement on the cylinder with the cone pres-
sure for the separation angle, $\alpha = 10^{\circ}$, is apparent, however.

The experimental heat-transfer results are presented in Fig. 14 and
compared with theory as noted in the figure. The nose cone heat transfer
falls above the laminar theory as found in the other results. The re-
sults on the cylinder upstream of transition are somewhat above laminar
theory for an attached flow on a cone defined by the separation angle.
The heat transfer on the cylinder downstream of transition is consider-
ably lower than turbulent theory for an attached flow on a cone defined
by the separation angle. The heat-transfer distribution and the magni-
tude compared with turbulent attached flow theory are similar to results
obtained by Larson (3) for a turbulent separation.

Tripped Boundary Layer

No separation of the turbulent attached boundary layer generated by
the nose cone trip was apparent. A representative pressure distribution
and the corresponding schlieren photograph are presented in Fig. 15; the
good agreement with theory is apparent. Representative heat-transfer re-
sults are shown in Fig. 16. The theoretical heat-transfer distributions
presented are from Reshotko and Tucker (14) for a turbulent attached
boundary layer starting at the tip of the nose cone and a turbulent
boundary layer starting at the cylinder-flare junction. The pressure
distribution assumed in the theory was the theoretical distribution for
the cone-cylinder and the cone value for the flares. Good agreement with
theory is observed generally for the cylinder heat transfer. For the
most part, the heat transfer on the flare follows more closely that pre-
dicted by theory for a turbulent boundary layer starting at the cylinder-
flare junction. The flare shock - boundary-layer interaction is there-
fore such that the turbulent boundary layer downstream of the shock is
quite thin, with the associated high heat-transfer rates. The schlieren
photographs also support this observation. The flare shock - boundary-
layer interaction for an attached turbulent boundary layer is therefore

similar to the reattachment shock - boundary-layer interaction found at reattachment for transitional separation.

CONCLUSIONS

Pure laminar and transitional separations and their effect on the overall heat transfer and pressure distributions on a cone-cylinder-flare configuration have been investigated experimentally at a Mach number of 5. The results presented allow the following conclusions:

1. The length of transitional separation decreases with wall cooling, decreasing flare angle, and increasing unit Reynolds number.

2. The pressure distribution across the separated region for separation of the cylinder boundary layer is well correlated by a plot of $(p/p_0 - 1)/\sqrt{(C_f)_0}$ against $(s/s_0 - 1)/\sqrt{(C_f)_0}$, where the subscript 0 indicates the start of interaction of separation on the pressure distribution.

3. The heat transfer on the flare afterbody is strongly dependent on the type of separation - pure laminar or transitional. Pure laminar separation exhibits the low heat transfer through reattachment associated with a laminar boundary layer. In transitional separation the reattachment shock - boundary-layer interaction is such that a thin turbulent boundary layer, with the associated high heating rates, occurs on the flare. Peak heating occurs in the reattachment region.

4. Separation induced by the large flare (56° half-angle) occurs directly off the nose cone and is markedly different from the separation obtained in the attached cylinder boundary-layer case. The pressure distribution on the cylinder is close to that predicted for a cone having a half-angle equal to the separation angle. The separation was transitional, and the heat transfer downstream of transition was considerably below turbulent theory for an attached flow on a cone defined by the edge of the separated region.

5. For an attached turbulent boundary layer with negligible separation, the flare shock - boundary-layer interaction is such that a thin turbulent boundary layer, with the associated high heating rates, occurs on the flare.

12

NOMENCLATURE

C_f	local skin friction coefficient (based on free-stream conditions)
C_p	pressure coefficient
c_p	specific heat at constant pressure
D	cylinder diameter
h	heat-transfer coefficient
l	length of separated region
p	pressure
p_p	plateau pressure in separated region
Re/ft	free-stream unit Reynolds number, ft^{-1}
Re_D	free-stream Reynolds number based on cylinder diameter
Re_l	free-stream Reynolds number based on length of separation
Re_s	free-stream Reynolds number based on surface distance
St	free-stream Stanton number
s	surface distance along model
T	temperature
t	time
x	axial distance along model
α	separation angle
θ	flare angle
ρ	density
τ_w	wall thickness

Subscripts:

aw   adiabatic wall

b   model material

cf   cylinder-flare junction

r   reattachment point

s   separation point

TR   transition

t   stagnation conditions

w   wall

O   start of interaction of separation on pressure distribution

REFERENCES

1. Chapman, D. R., Kuehn, D. M., and Larson, H. K., "Investigation of Separated Flows in Supersonic and Subsonic Streams with Emphasis on the Effect of Transition," NACA Rep. 1356, 1958. (Supersedes NACA TN 3869.)

2. Chapman, D. R., "A Theoretical Analysis of Heat Transfer in Regions of Separated Flow," NACA TN 3792, 1956.

3. Larson, H. K., "Heat Transfer in Separated Flows," Jour. Aero/Space Sci., vol. 26, no. 11, Nov. 1959, pp. 731-738.

4. Stalder, J. R., and Nielsen, H. V., "Heat Transfer from a Hemisphere-Cylinder Equipped with Flow-Separation Spikes," NACA TN 3287, 1954.

5. Crawford, D. H., "Investigation of the Flow Over a Spike-Nose Hemisphere-Cylinder at a Mach Number of 6.8," NASA TN D-118, 1959.

6. Powers, W. E., Stetson, K. F., and Adams, M. C., "A Shock Tube Investigation of Heat Transfer in the Wake of a Hemisphere-Cylinder, with Application to Hypersonic Flight," AVCO Research Report 30 (IAS Report No. 59-35), 1959.

7. Larson H. K., and Keating, S. J., "Transition Reynolds Numbers of Separated Flows at Supersonic Speeds," NASA TN D-349, 1960.

14

8. Jack, J. R., and Diaconis, N. S., "Heat-Transfer Measurements on Two Bodies of Revolution at a Mach Number of 3.12," NACA TN 3776, 1956.

9. Cohen, C. B., and Reshotko, E., "The Compressible Laminar Boundary Layer with Heat Transfer and Arbitrary Pressure Gradient," NACA Rep. 1294, 1956. (Supersedes NACA TN 3326.)

10. Reshotko, E., "Simplified Method for Estimating Compressible Laminar Heat Transfer with Pressure Gradient," NACA TN 3888, 1956.

11. Clippinger, R. F., Giese, J. H., and Carter, W. C., "Tables of Supersonic Flows about Cone Cylinders," Part I: Surface Data. B.R.L. Report 729, 1950.

12. Jack, J. R., "Theoretical Wave Drags and Pressure Distributions for Axially Symmetric Open-Hose Bodies," NACA TN 2115, 1950.

13. Ames Research Staff, "Equations, Tables, and Charts for Compressible Flow," NACA Rep. 1135, 1953. (Supersedes NACA Rep. 1428.)

14. Reshotko, E., and Tucker, M., "Approximate Calculation of the Compressible Turbulent Boundary Layer with Heat Transfer and Arbitrary Pressure Gradient," NACA TN 4154, 1957.

Thermocouple and Pressure Tap Locations at Axial Distance x, in.

Cone-cylinder													
1.45	4.27	5.27	6.27	6.77*	7.27	7.78*	8.27	8.78*	9.27	9.77*	10.27	10.83	11.15

*Pressure tap only

10° Flare									
11.39	11.88	12.38	13.04	13.69	14.37	15.01	15.68	16.34	16.99

17° Flare								
11.40	11.88	12.34	12.98	13.61	14.25	14.90	15.53	16.49

24° Flare								
11.38	11.84	12.30	12.76	13.20	13.65	14.10	14.56

56° Flare				
11.37	11.51	11.79	12.06	12.34
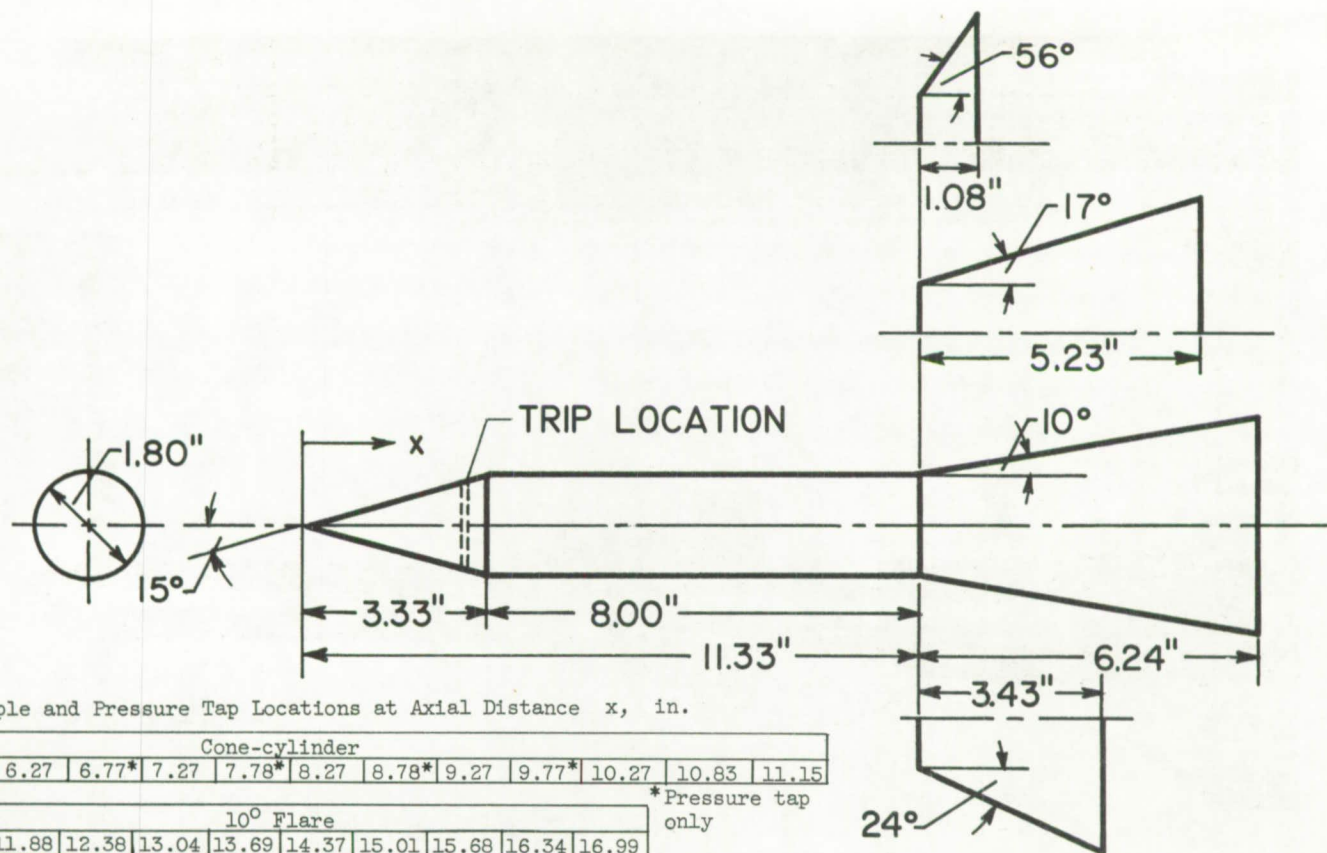
Fig 1 Model dimensions, and thermocouple and pressure tap locations

COOLING SHOE

FLARE ($\theta = 17°$)

CONE-CYLINDER

C-56704
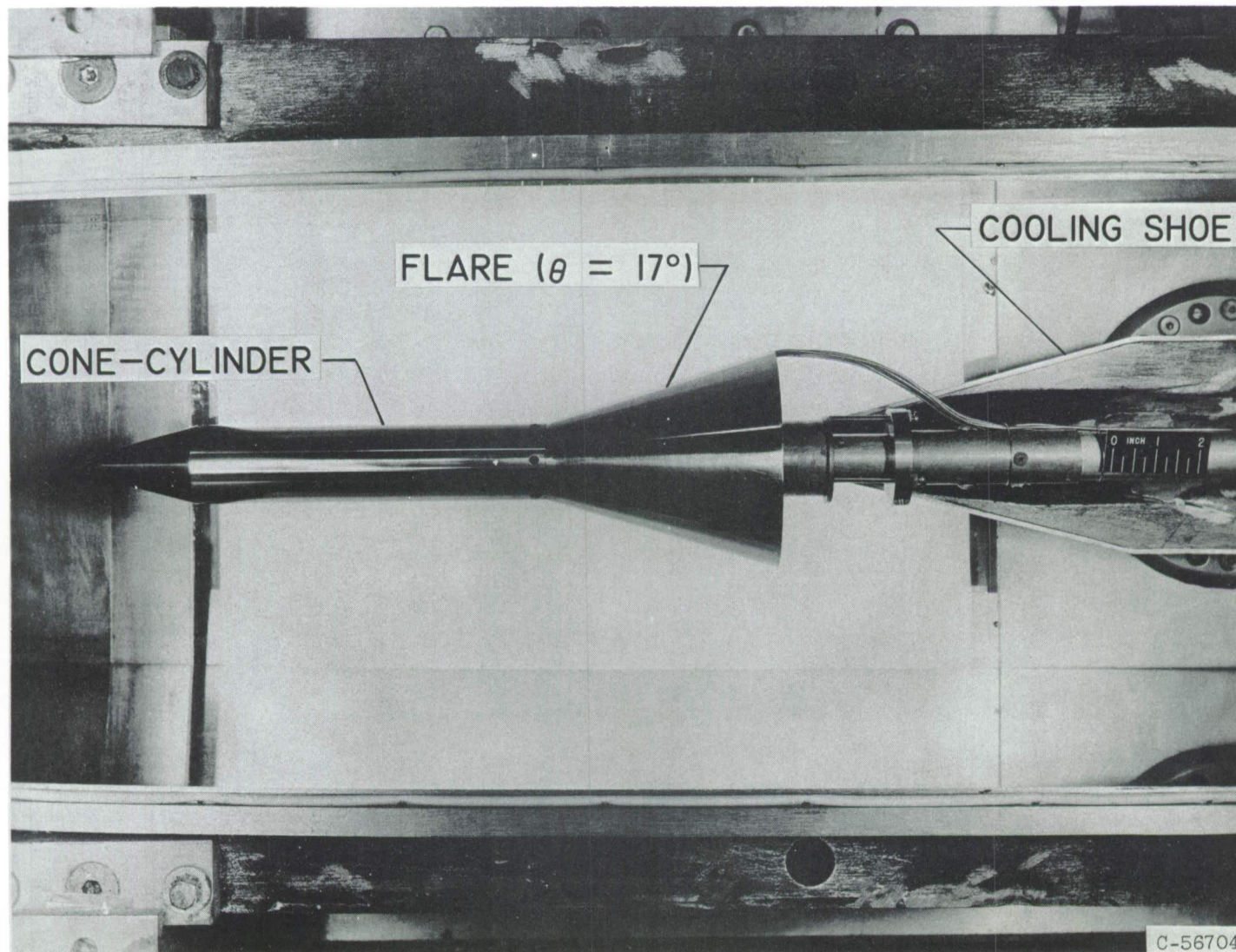
Fig 2 Tunnel installation. Model in test position; cooling shoes retracted
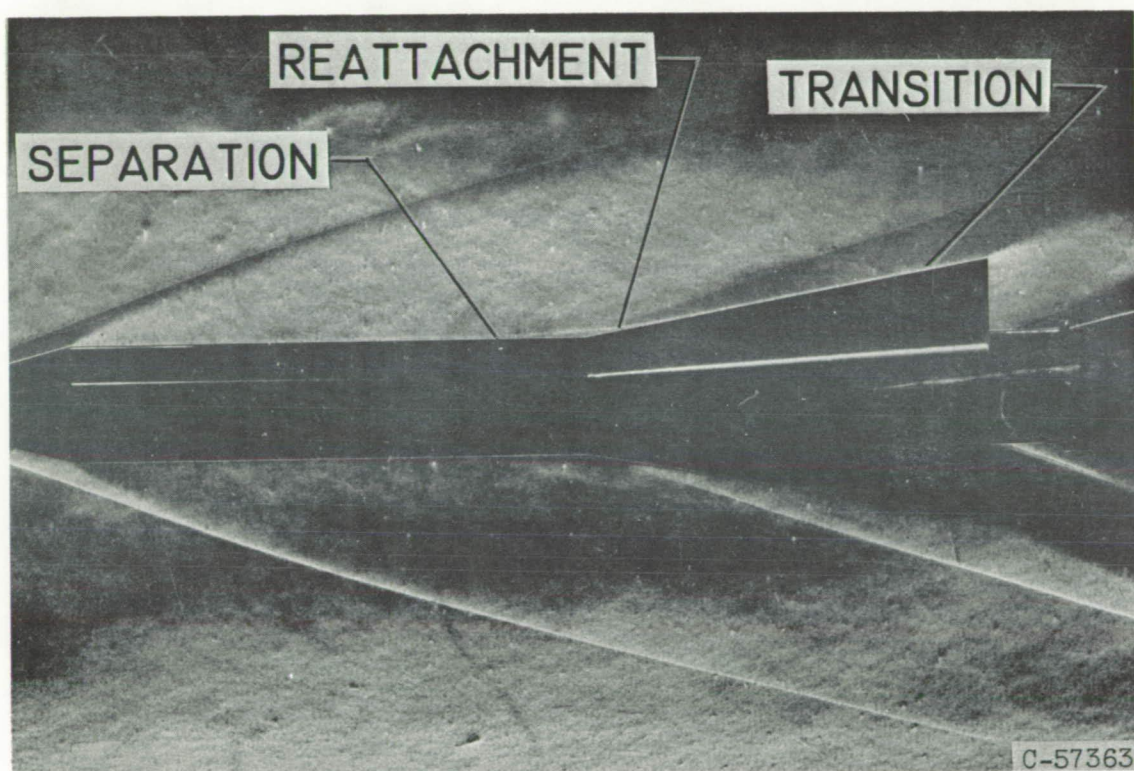
Fig 3 Pure laminar separation. $\theta = 10^{\circ}$; Re/ft = 1.9×10^6;
$(T_w/T_t)_s = 0.23$; $(T_w/T_t)_{TR} = 0.40$
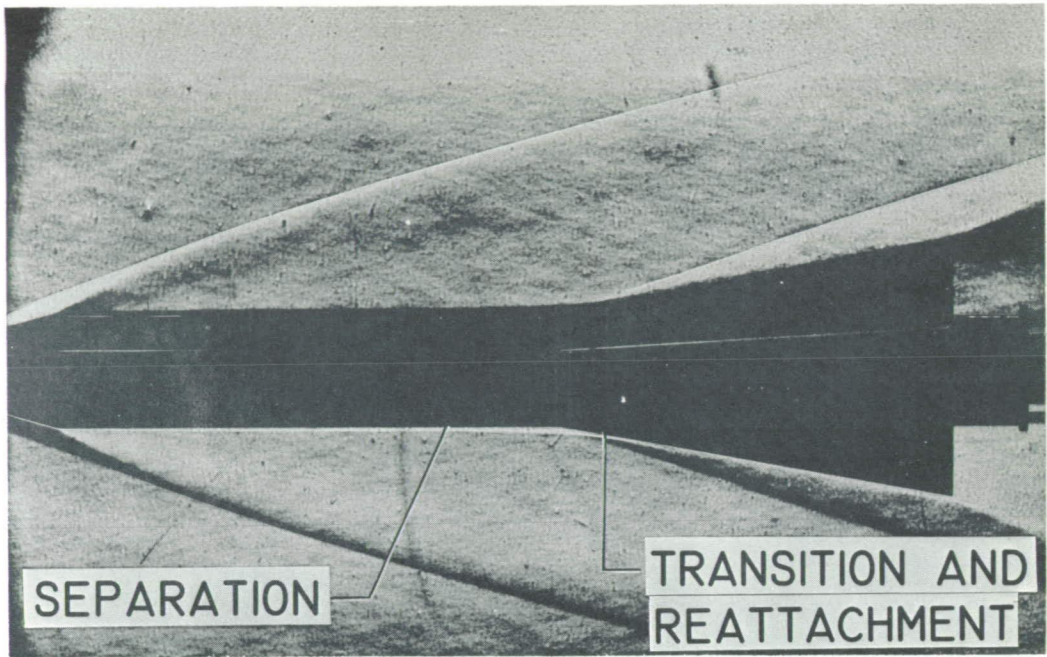
(a) $\theta = 10^{\circ}$; $Re/ft = 5.4 \times 10^{6}$; T_w/T_t = adiabatic
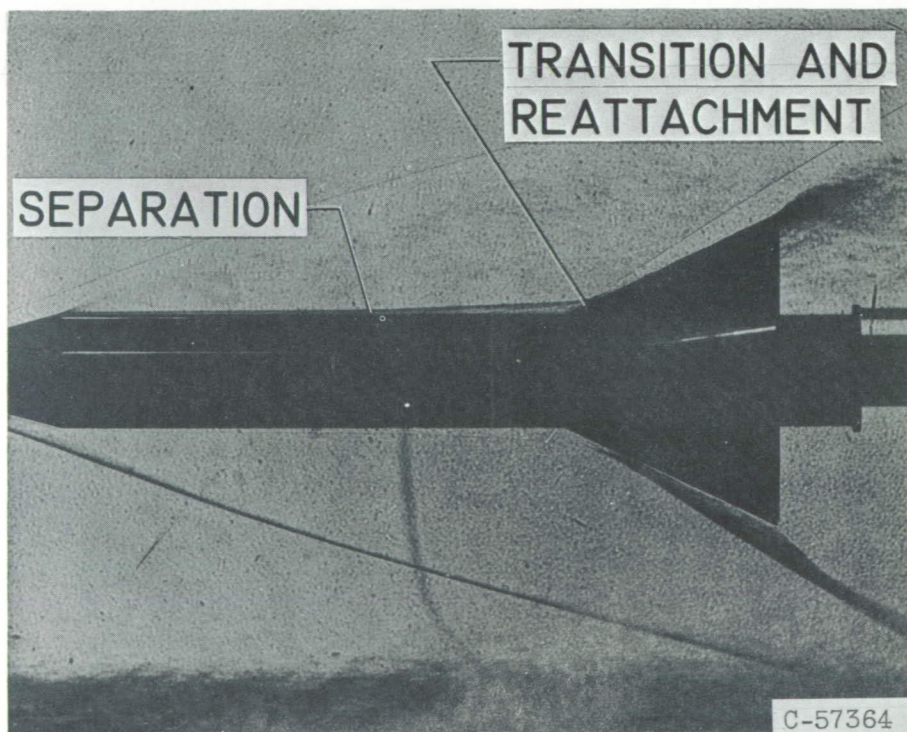
(b) $\theta = 24^{\circ}$; $Re/ft = 5.4 \times 10^{6}$; T_w/T_t = adiabatic

Fig 4   Transitional separation
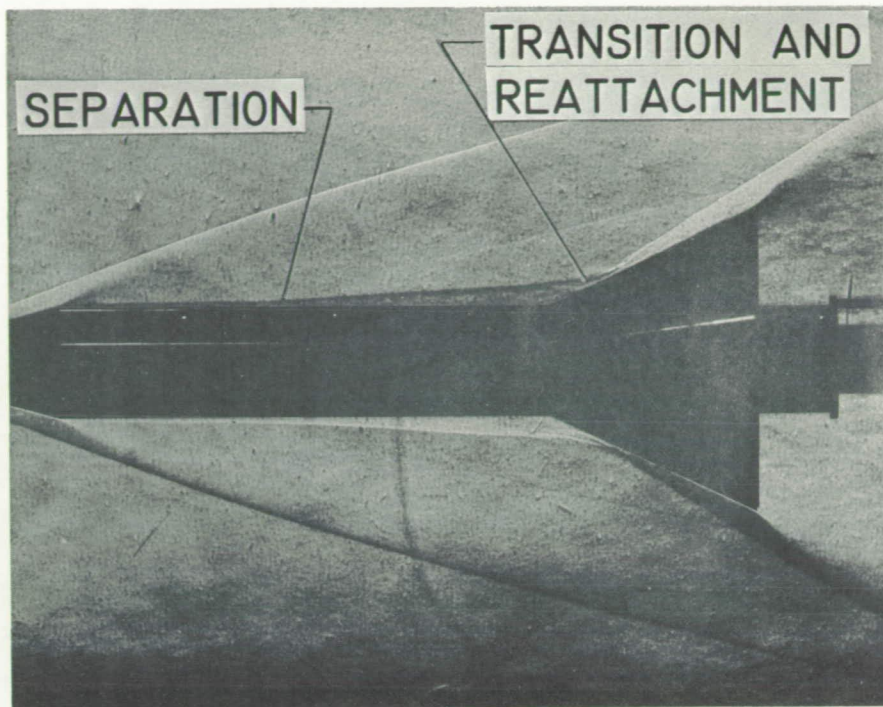
(c) $\theta = 24^{\circ}$; $Re/ft = 2.6 \times 10^{6}$; T_w/T_t = adiabatic
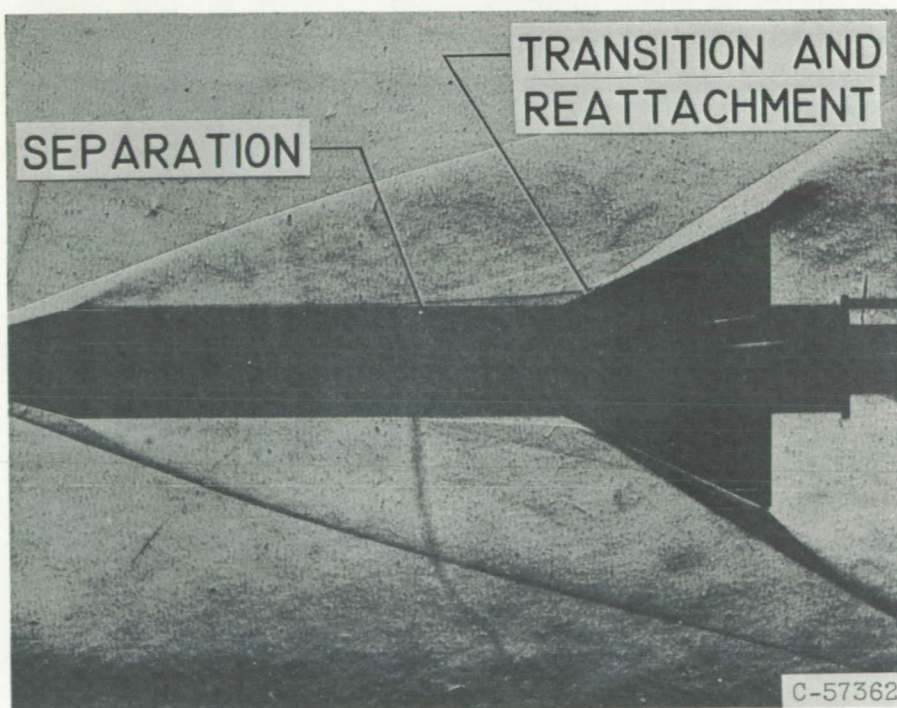
(d) $\theta = 24^{\circ}$; $Re/ft = 2.6 \times 10^{6}$; $(T_w/T_t)_s = 0.18$

Fig 4 Concluded Transitional separation
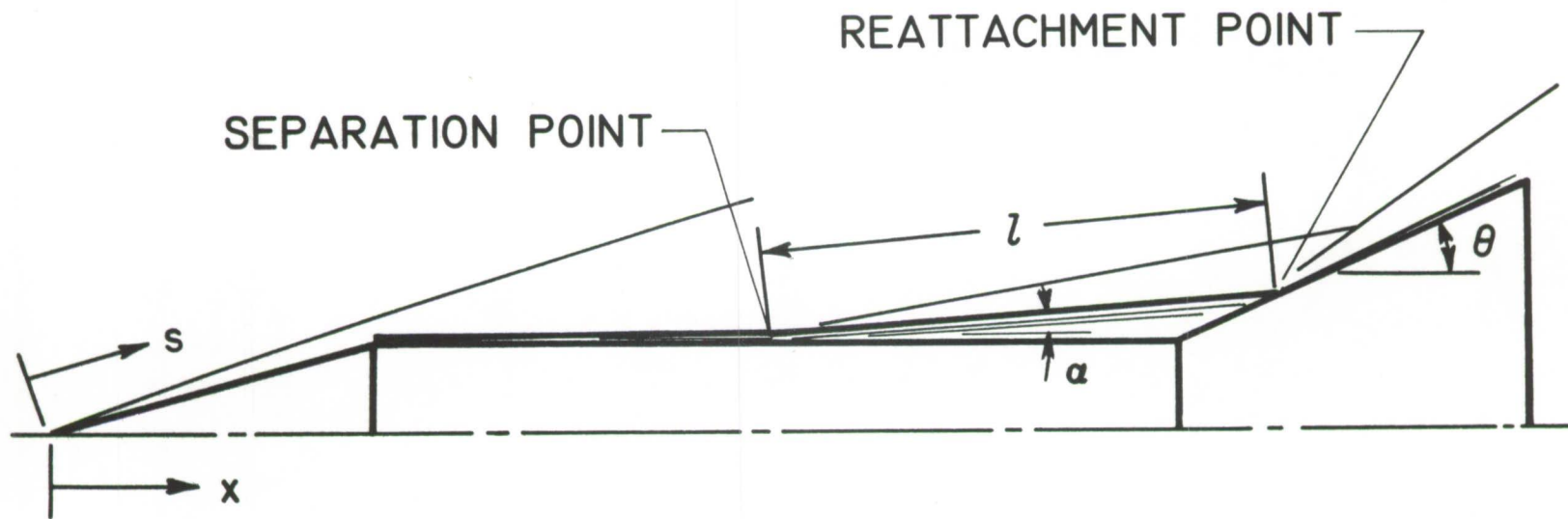
Fig 5   Separation geometry variables

Fig 6 Effect of unit Reynolds number and flare angle on sep-
aration geometry
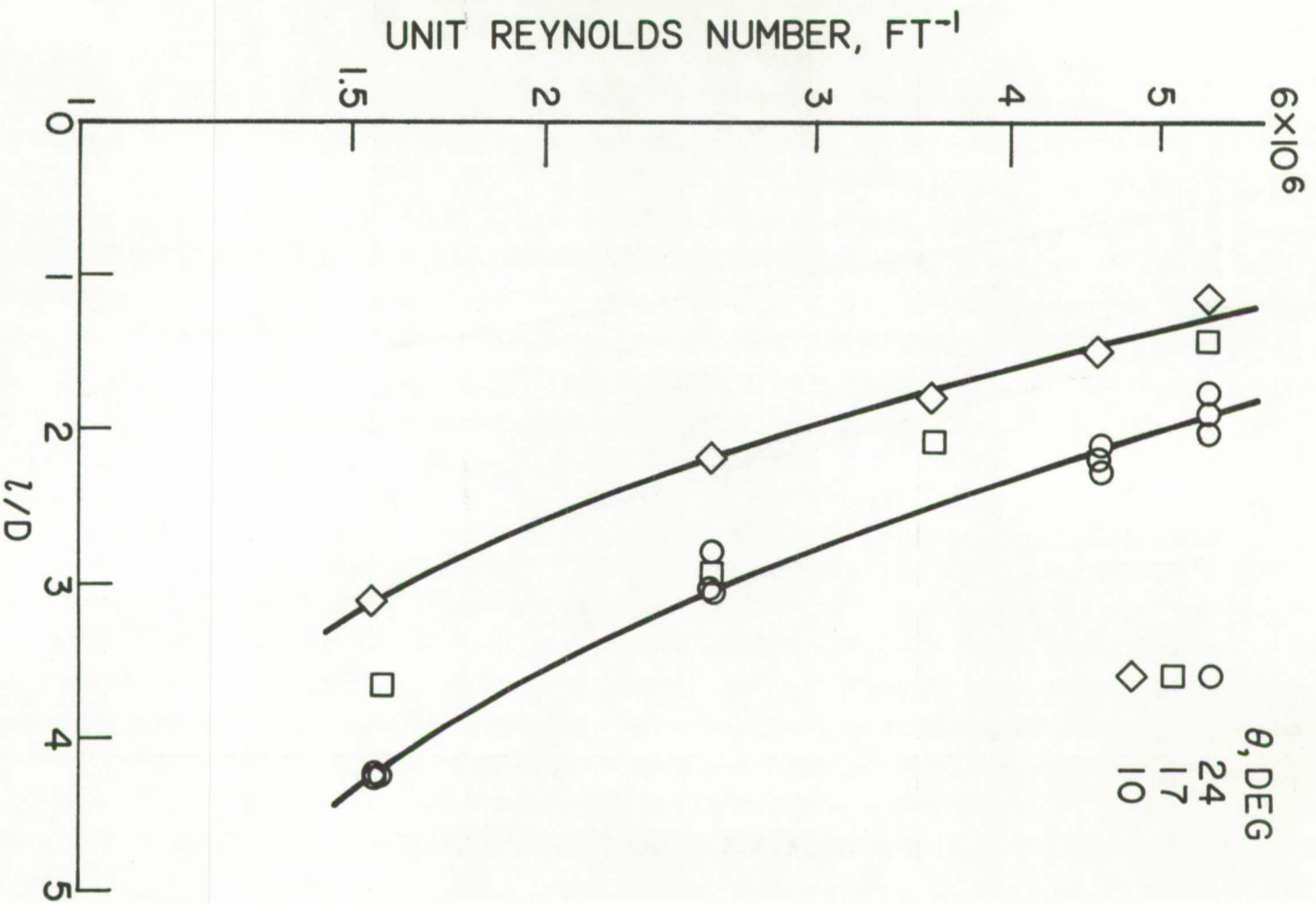
(a) Length of separation; T_w/T_t = adiabatic
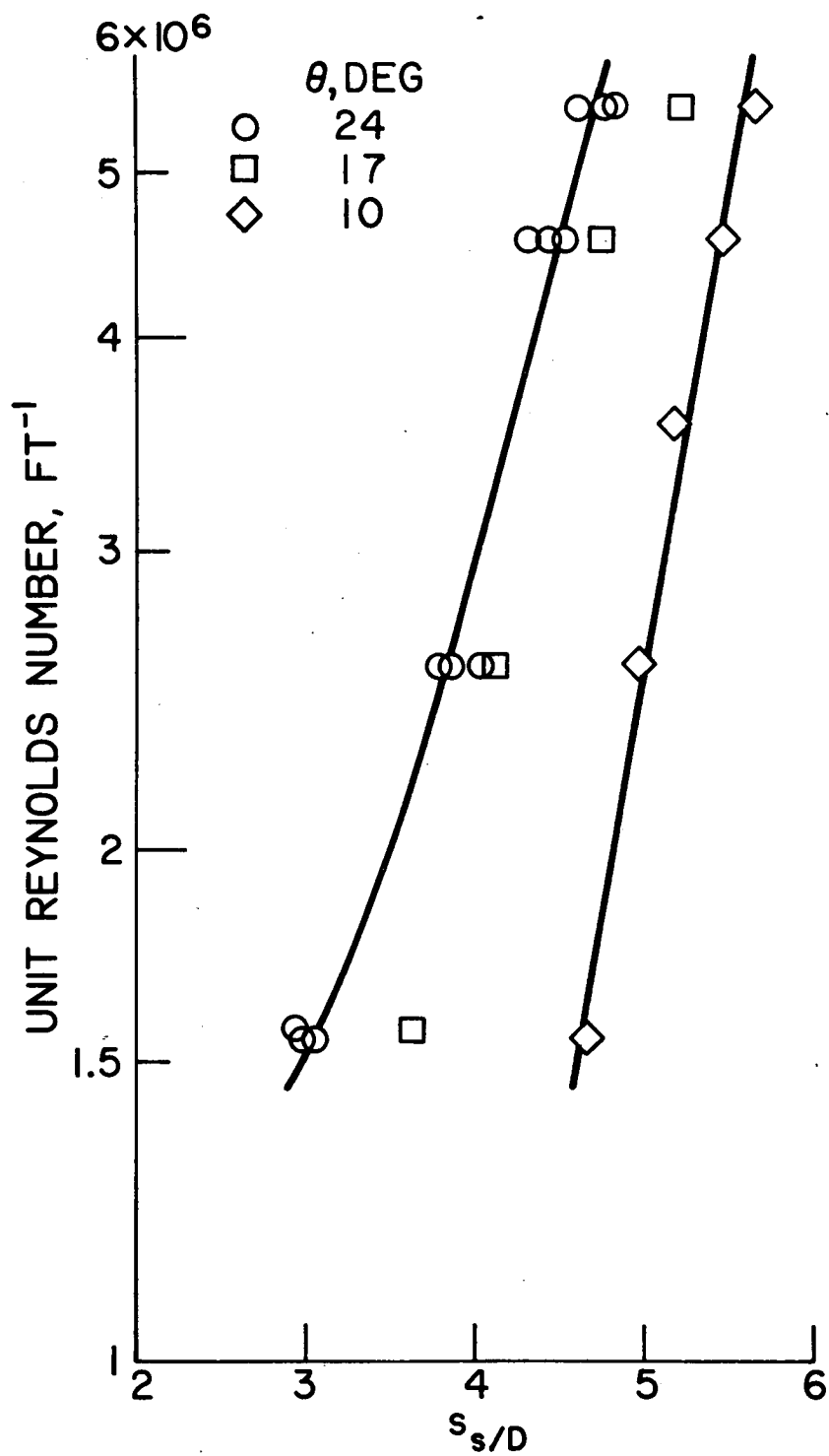
(b) Distance to separation; T_w/T_t = adiabatic

Fig 6 Concluded   Effect of unit Reynolds number and
flare angle on separation geometry
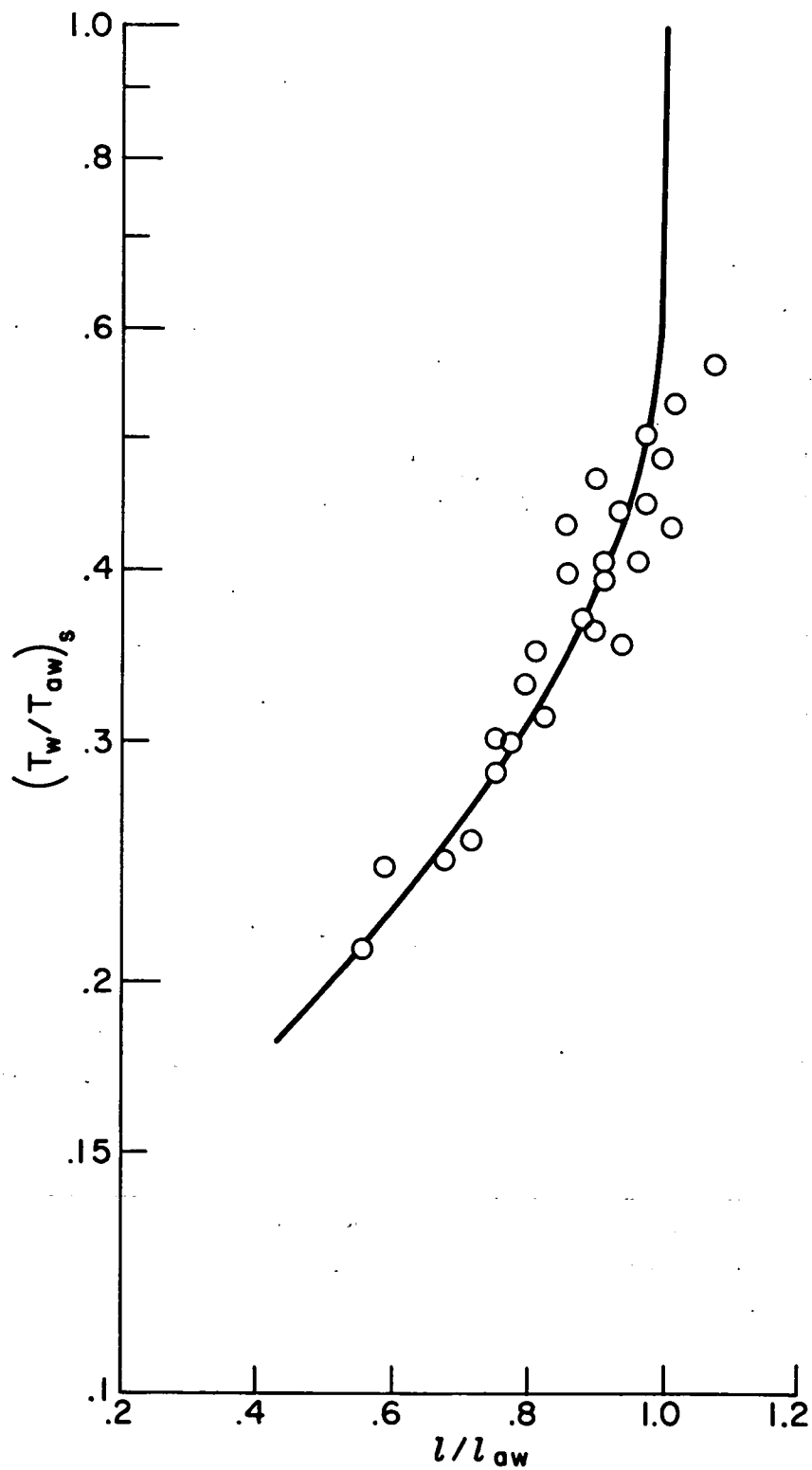
Fig 7 Effect of wall cooling on the length of separation.
$\theta = 24^\circ$; $1.6 \times 10^6 \leq Re/ft \leq 5.4 \times 10^6$
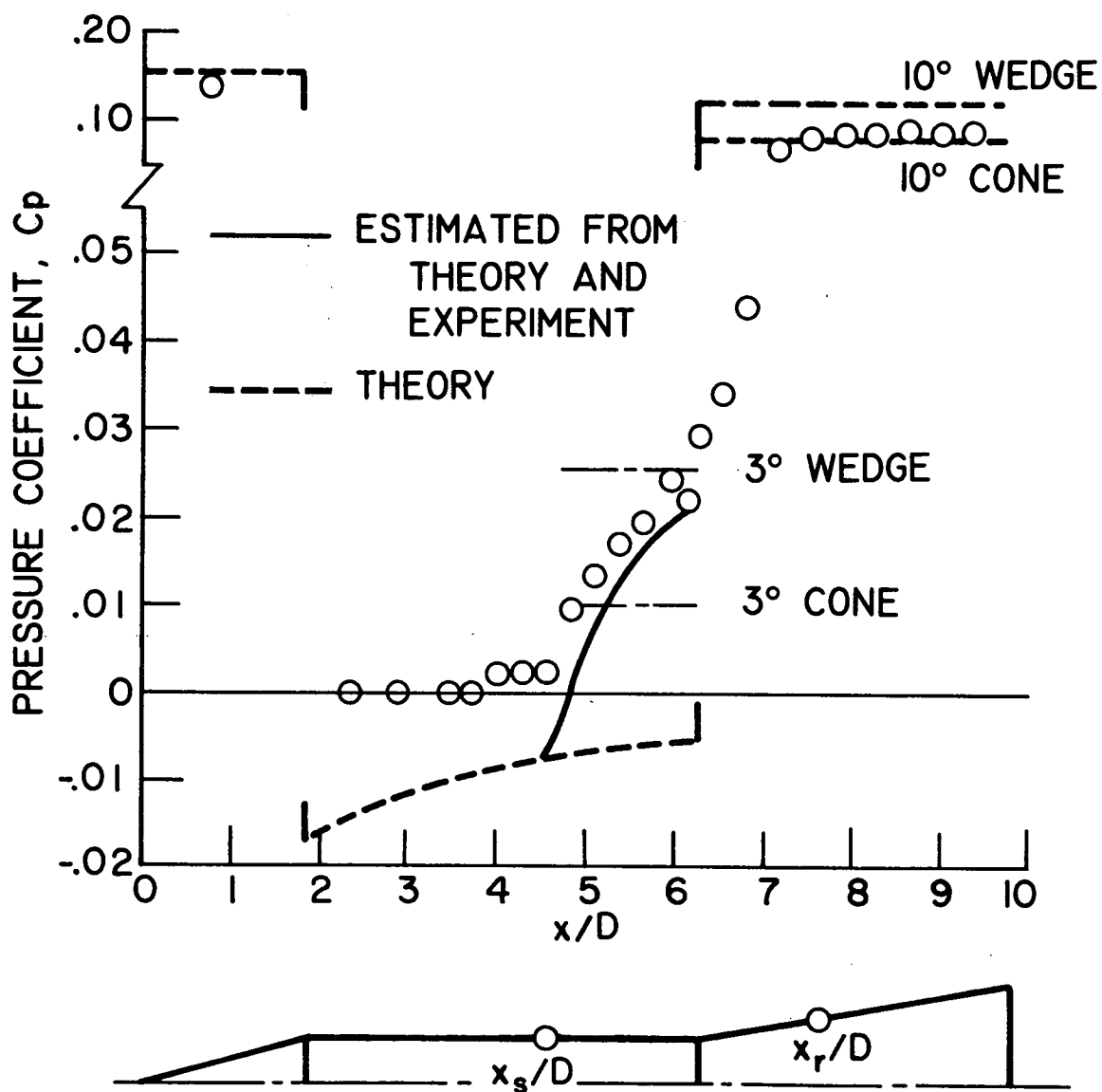
Fig 8 Pressure distribution, pure laminar separation. $\theta = 10^{o}$; Re/ft = 1.6×10^{6}; T_w/T_t = adiabatic
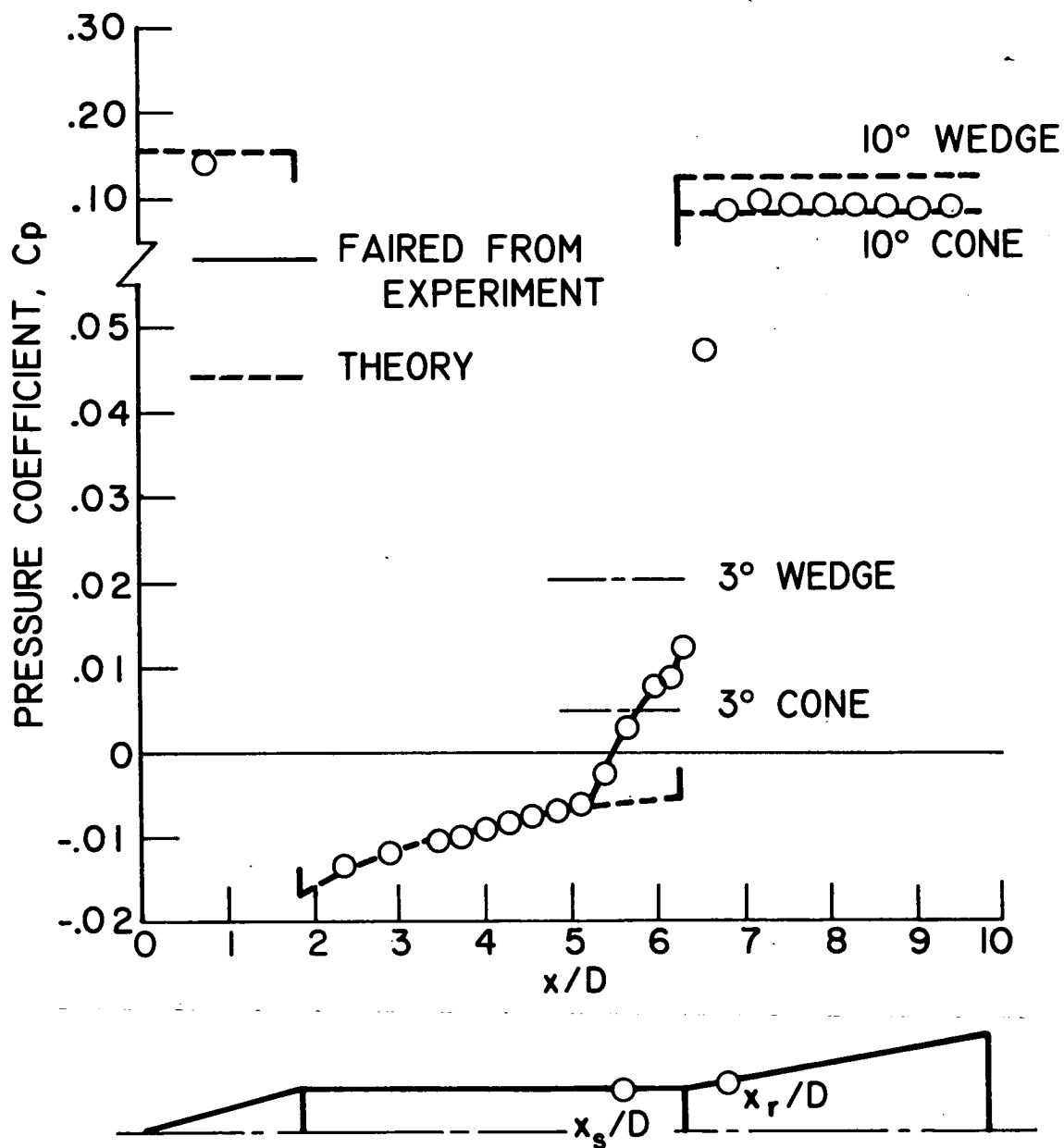
(a) $\theta = 10^{\circ}$; Re/ft = 5.4×10^6; T_w/T_t = adiabatic

Fig 9 Pressure distribution, transitional separation
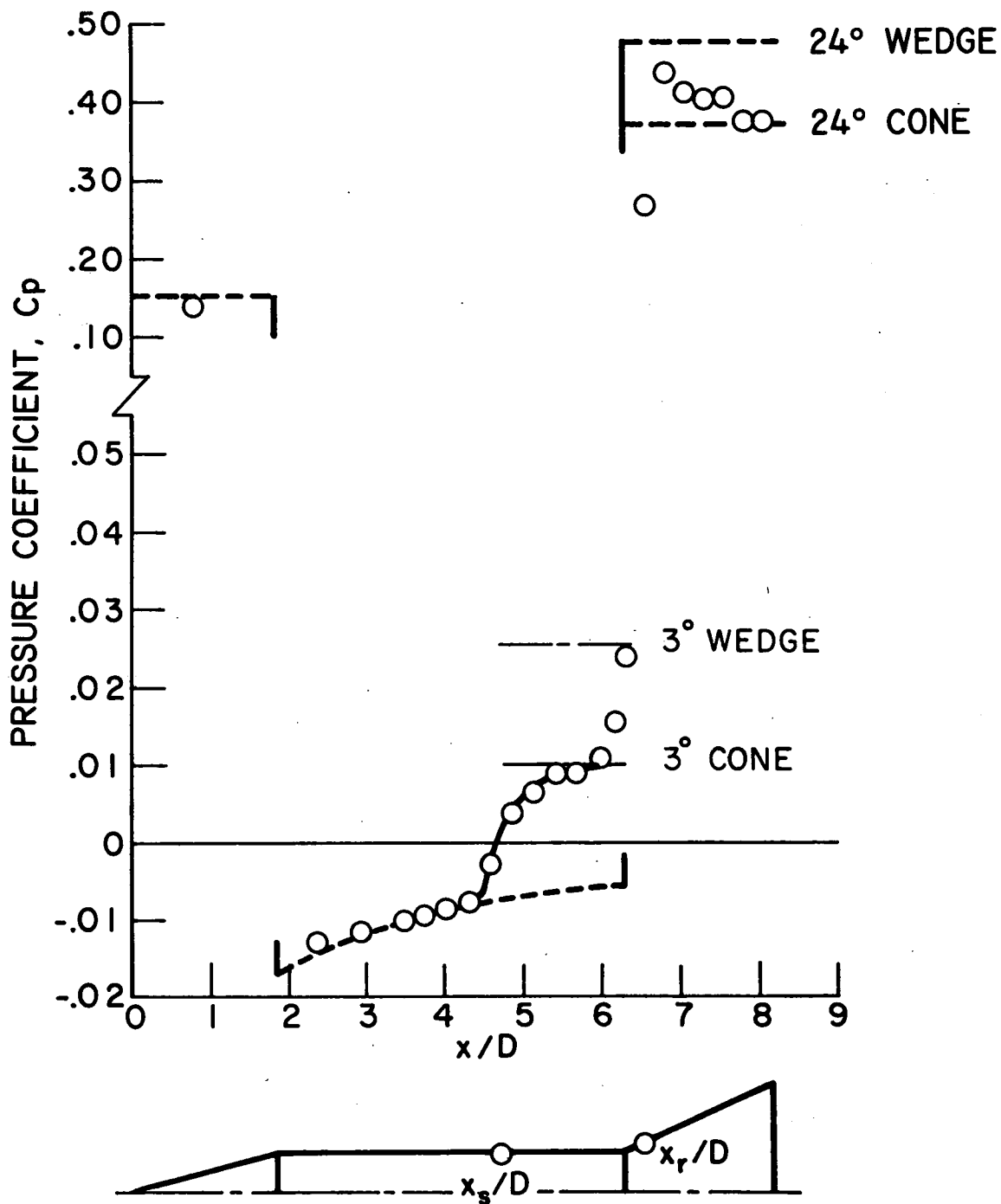
(b) $\theta = 24°$; Re/ft = 5.4×10^6; T_w/T_t = adiabatic

Fig 9 Concluded Pressure distribution, transitional separation
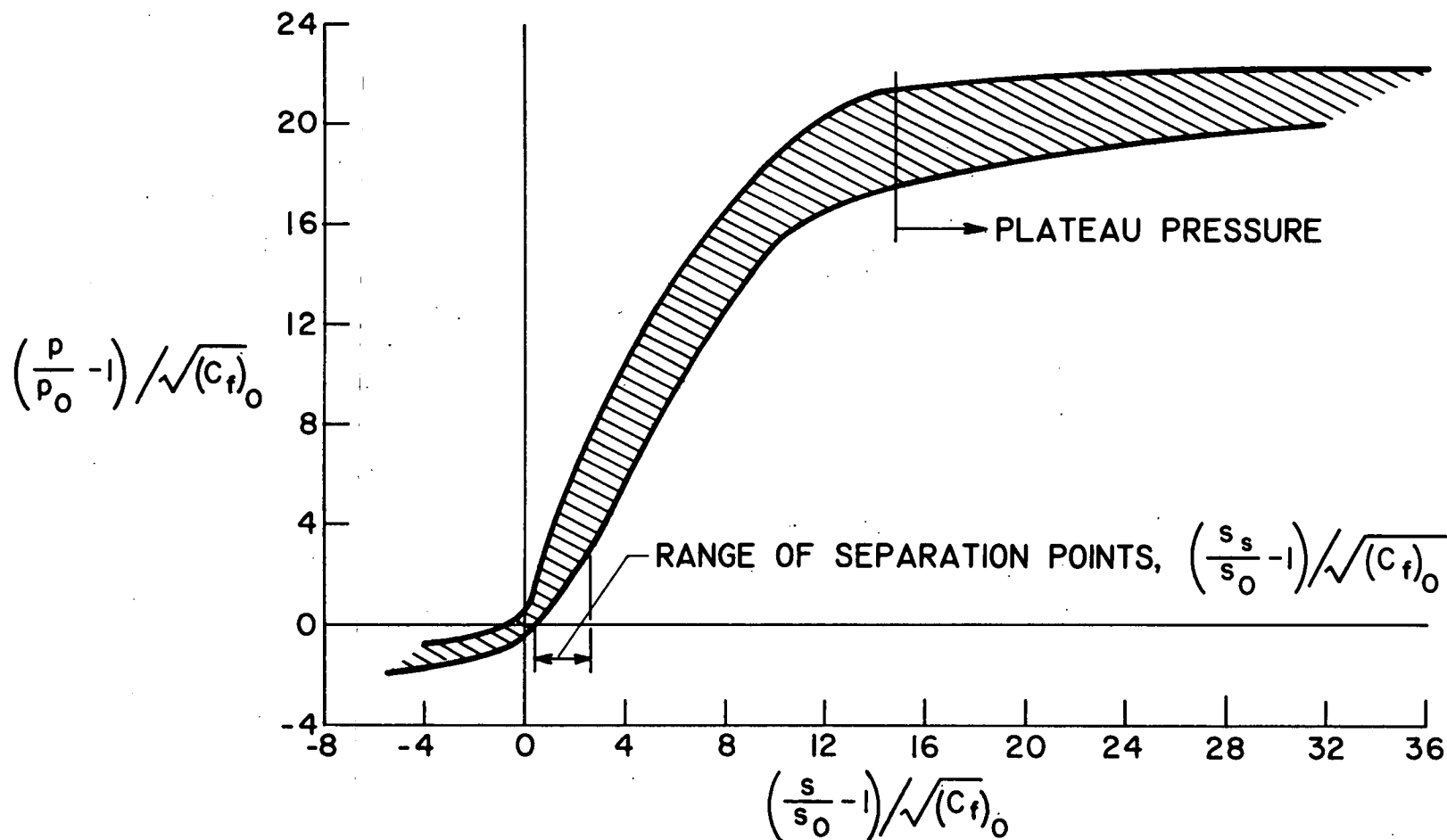
Fig 10 Correlation of the pressure distribution across the separated region, pure laminar and transitional separations. $\theta = 10^{\circ}$, 17°, and 24°, $1.6 \times 10^{6} \le Re/ft \le 5.4 \times 10^{6}$; T_w/T_t = adiabatic
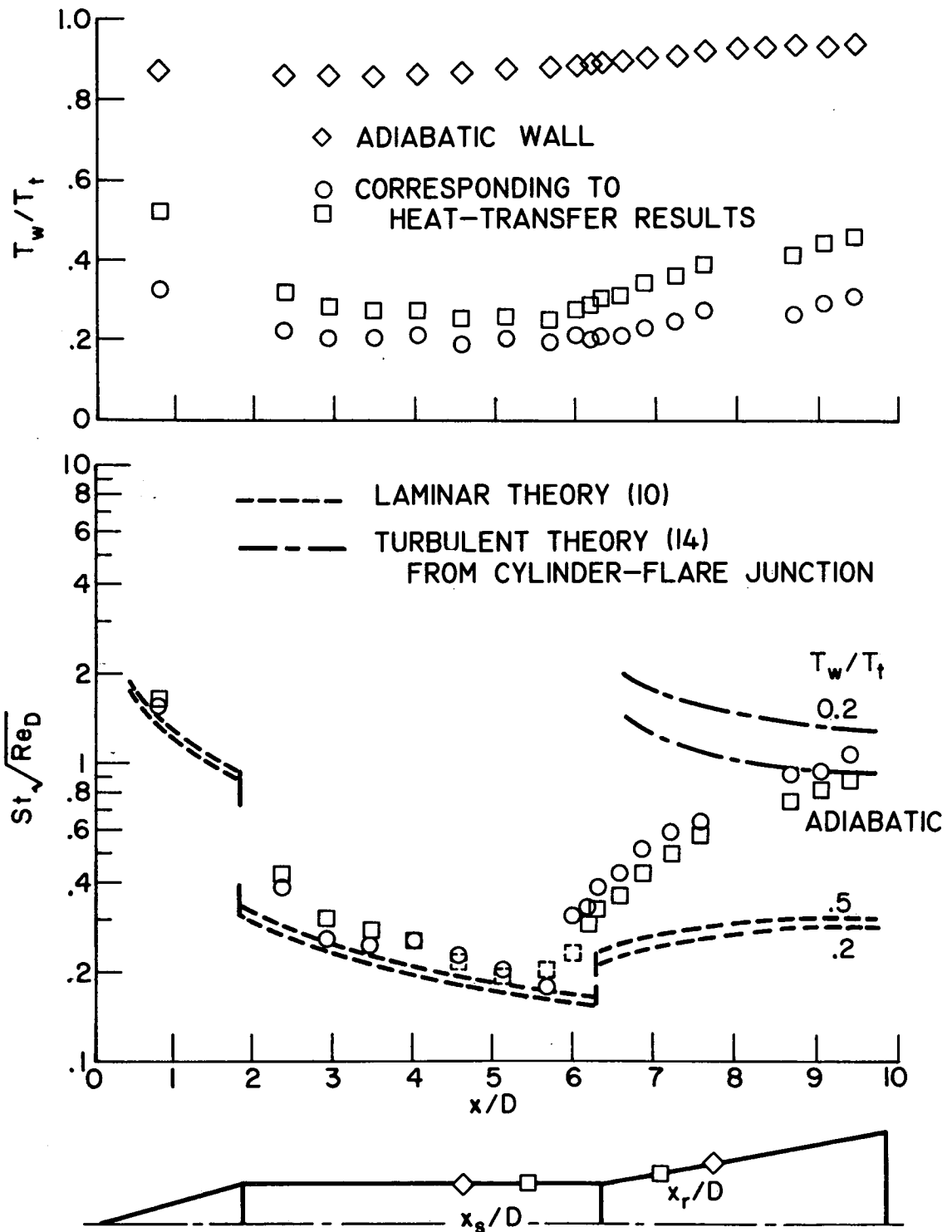
Fig 11 Heat transfer, pure laminar separation. $\theta = 10^{\circ}$; Re/ft $= 1.6 \times 10^6$; $Re_D = 0.24 \times 10^6$
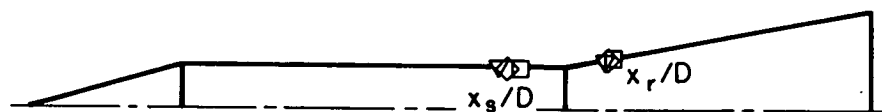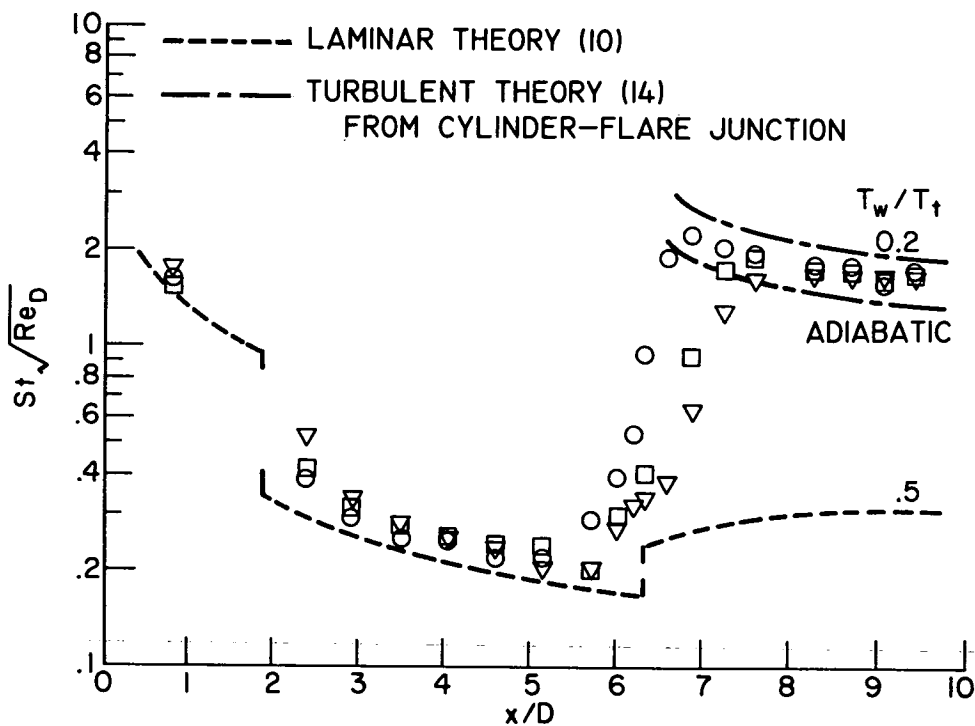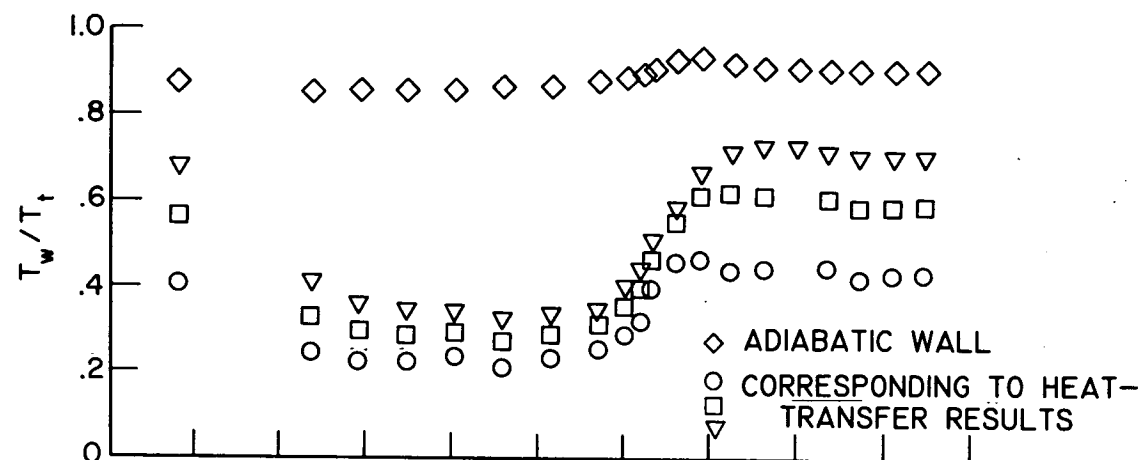
(a) $\theta = 10°$; Re/ft $= 5.4 \times 10^6$; $Re_D = 0.81 \times 10^6$

Fig 12 Heat transfer, transitional separation
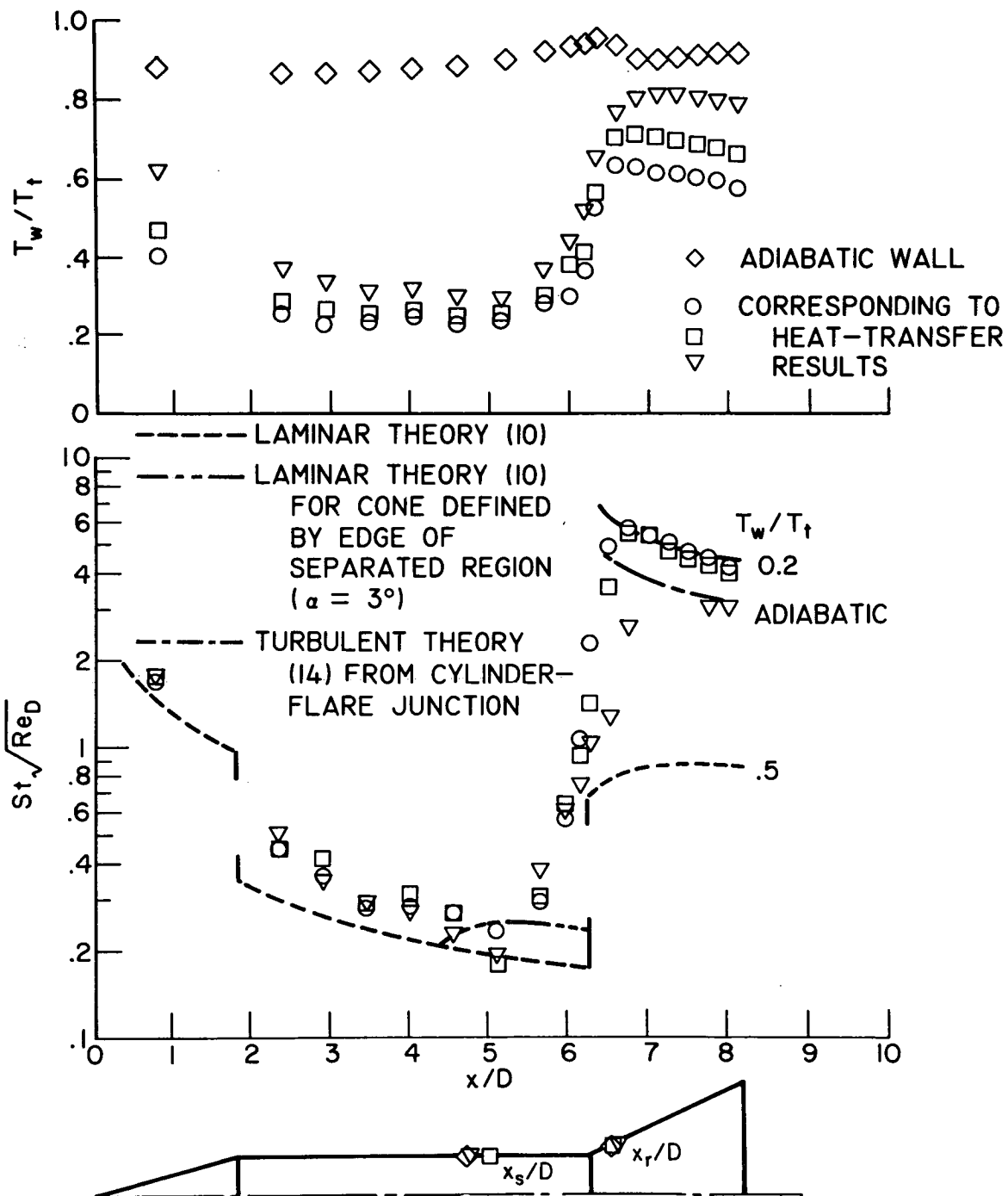
(b) $\theta = 24°$; $Re/ft = 5.4 \times 10^6$; $Re_D = 0.81 \times 10^6$

Fig 12 Concluded Heat transfer, transitional separation
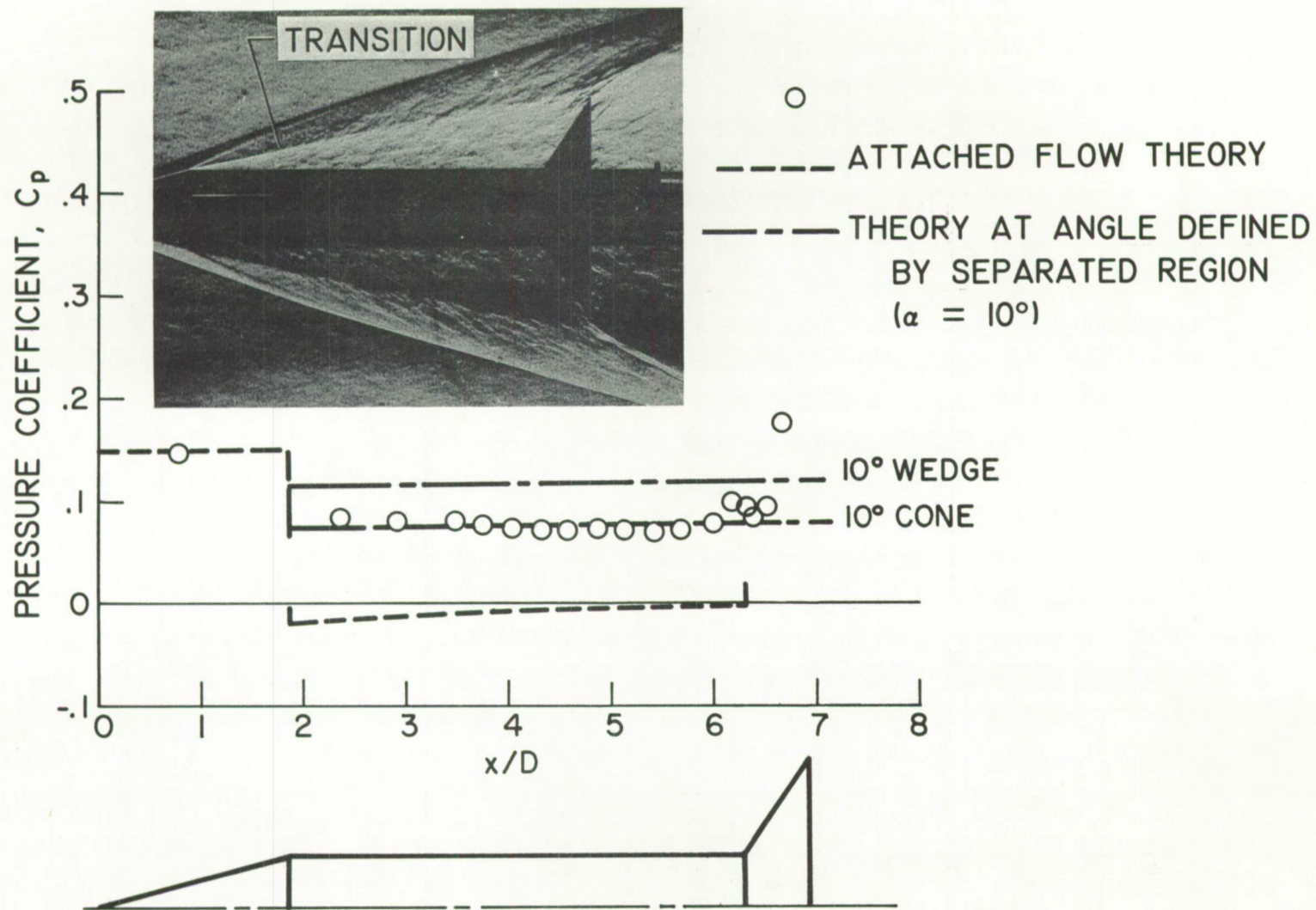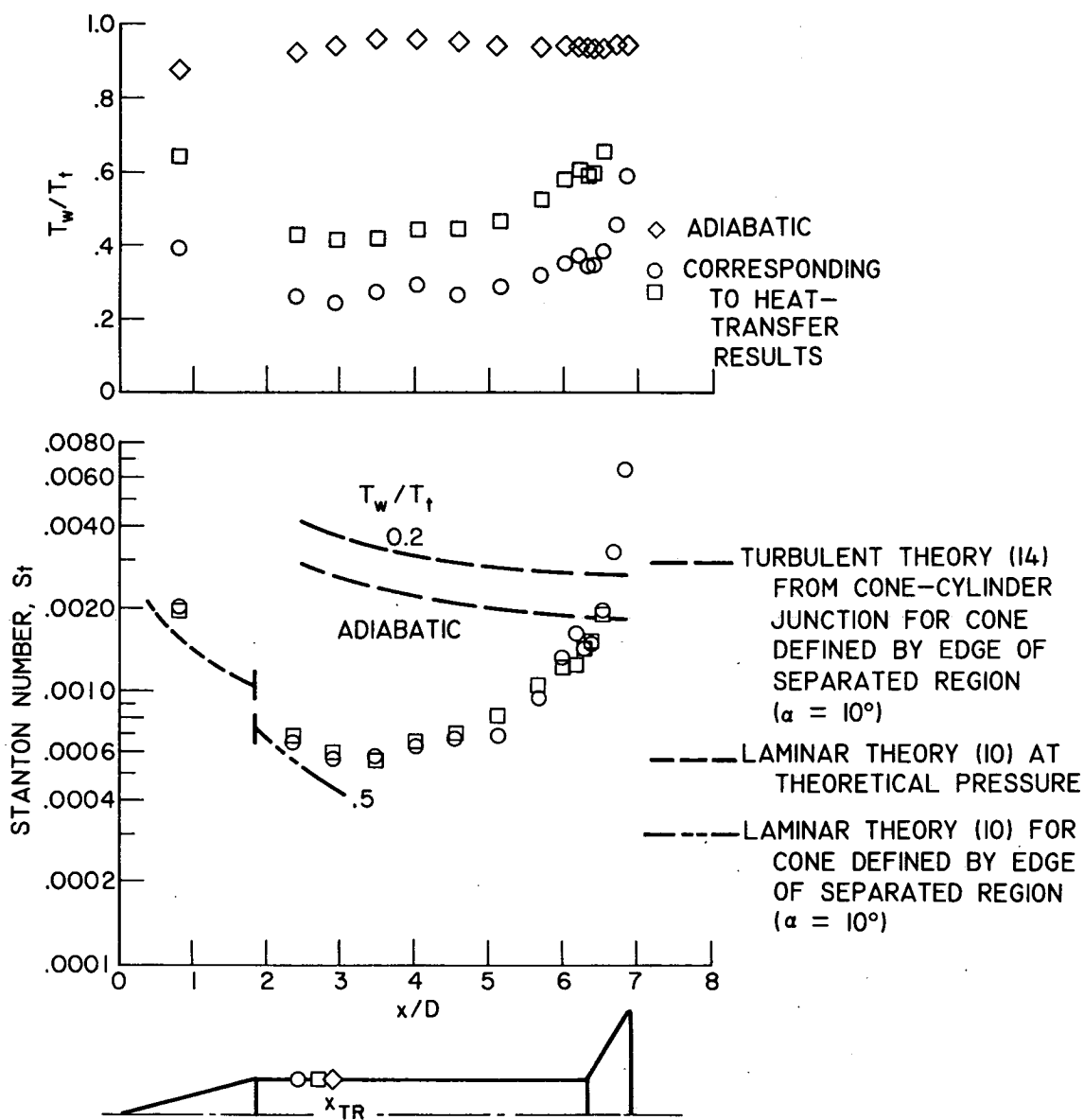
Fig 13 Pressure distribution, 56° flare. Re/ft = 5.4x10⁶

Fig 14 Heat transfer, 56° flare. Re/ft = 5.4×10⁶

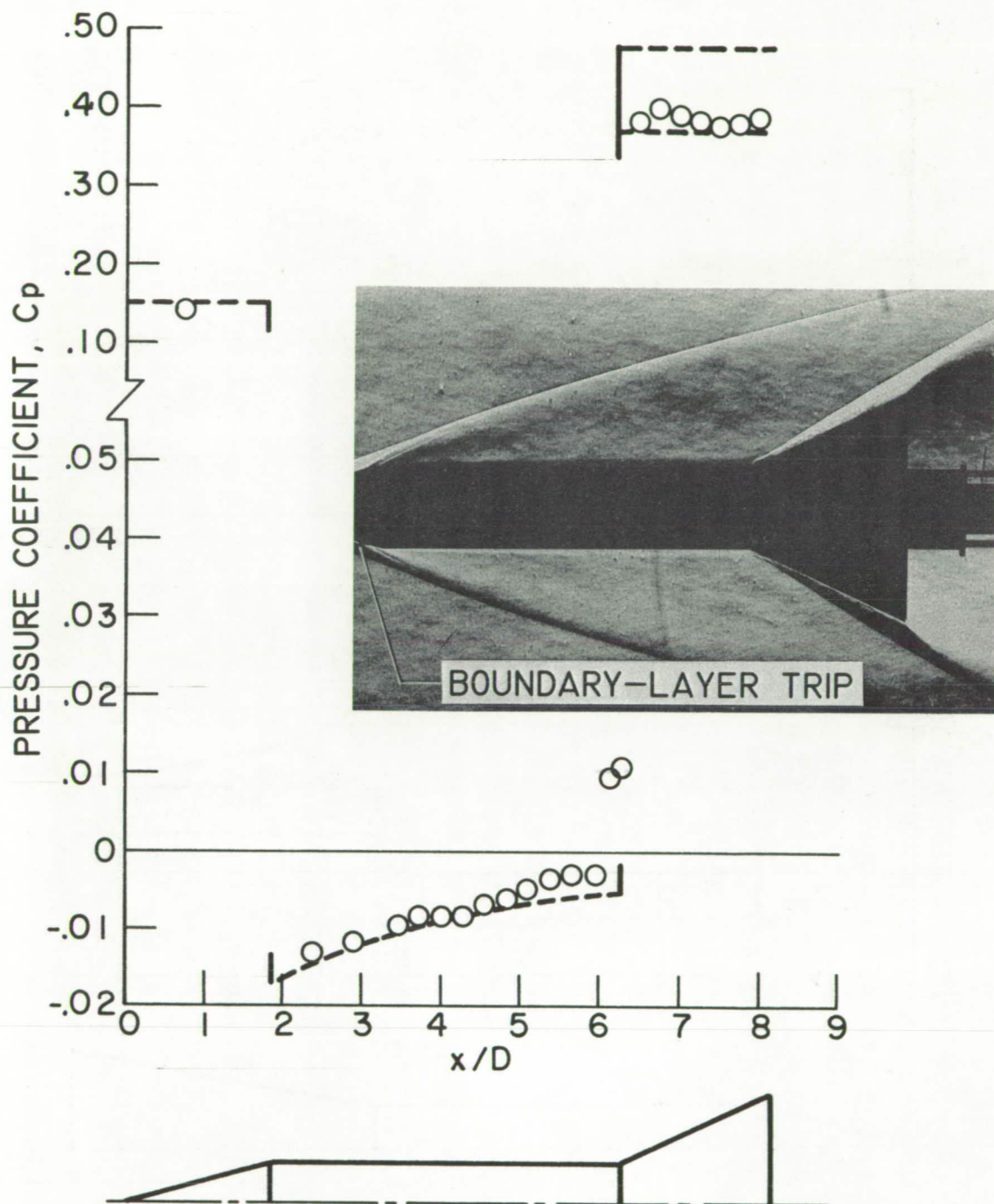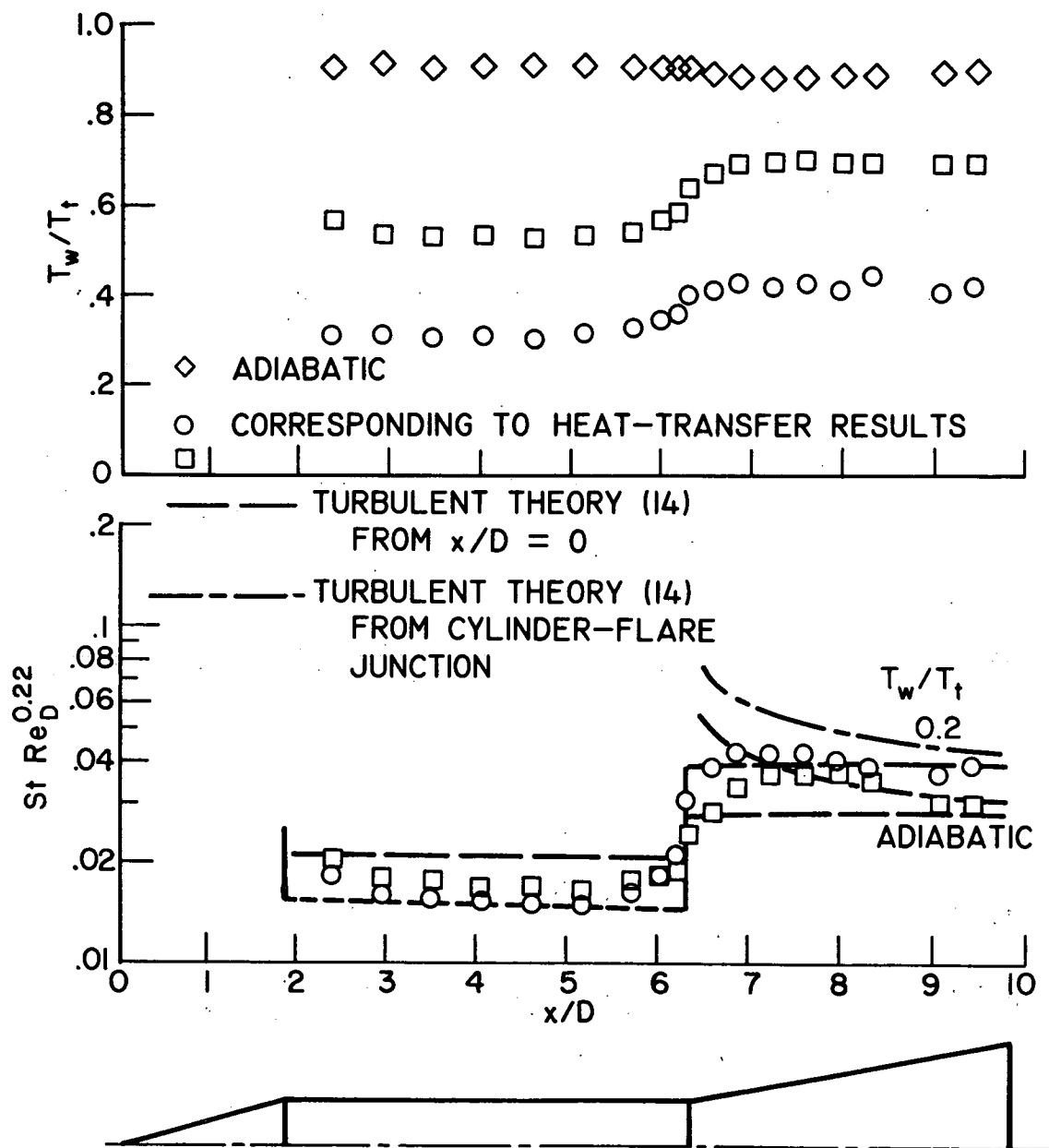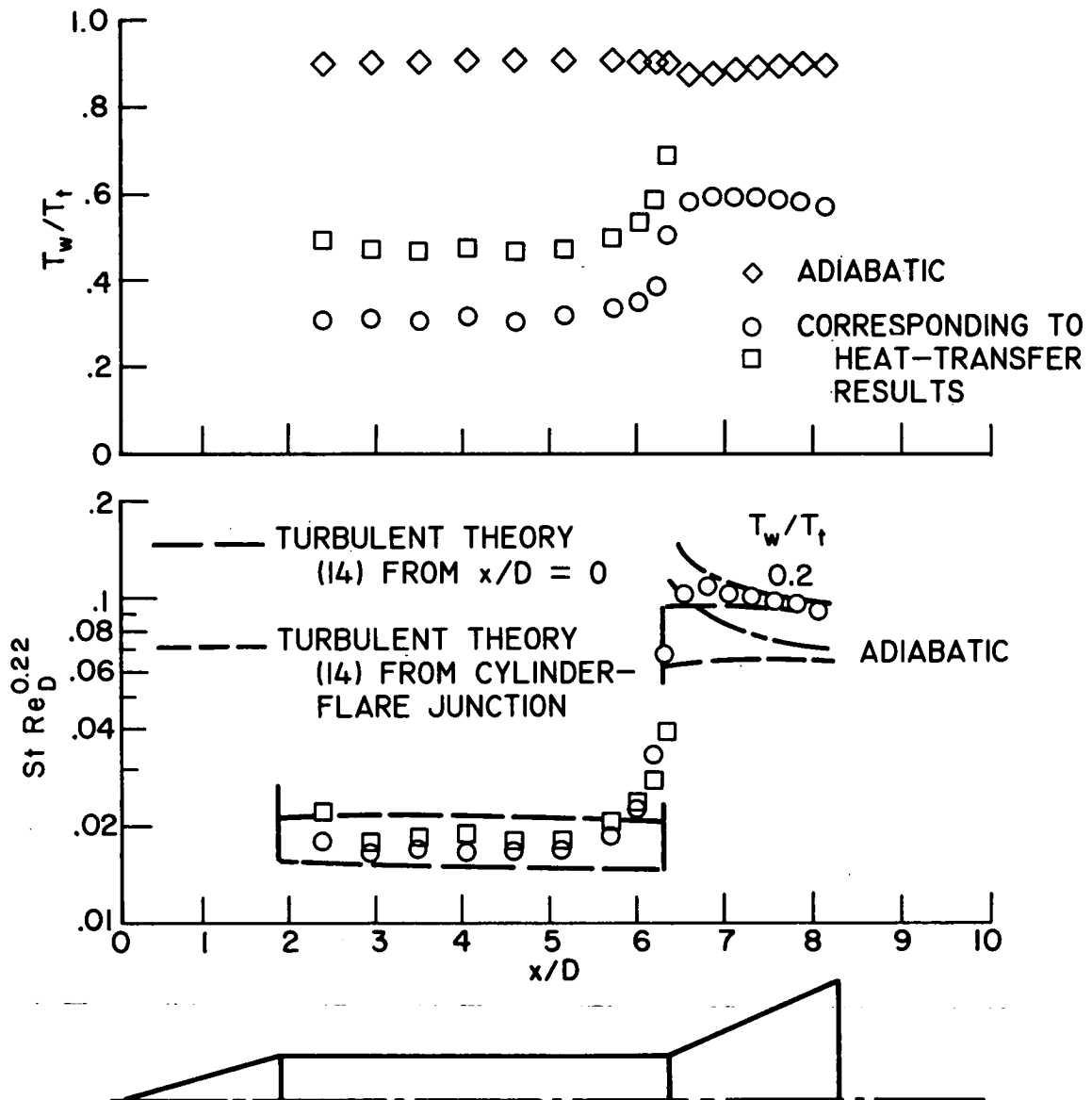Fig 15 Pressure distribution, tripped boundary layer. $\theta = 24^{\circ}$;
Re/ft = 5.4x10^6; T_w/T_t = adiabatic

(a) $\theta = 10^{\circ}$; Re/ft = 5.4x10^6; Re$_D$ = 0.81x10^6

Fig 16 Heat transfer, tripped boundary layer

(b) $\theta = 24°$; Re/ft $= 5.4 \times 10^6$; Re$_D = 0.81 \times 10^6$

Fig 16 Concluded Heat transfer, tripped boundary layer